SILT TRANSPORT BY THIN FILM FLOW

Thesis for the Degree of M. S. MICHIGAN STATE UNIVERSITY TERENCE HUGH PODMORE 1969

THESIS

LIBPARY
Michigan State
University

ABSTRACT

SILT TRANSPORT BY THIN FILM FLOW

Ву

Terence Hugh Podmore

Advances in soil conservation and erosion control depend upon the knowledge of the mechanics of the processes involved. Considerable research has been done in the last 20 years on splash erosion, and on the transport of eroded material by open channel flow. Little work has been done on the processes by which eroded material is transported from its place of detachment to a body of water moving with sufficient velocity to prevent sedimentation.

This work was performed to investigate the transport capabilities of uniformly flowing films of water simulating overland flow on a watershed during the runoff process. The variables considered were: slope, flow rate, surface roughness, distance the eroded material was transported before deposition occurred, and the proportion of material deposited as a function of particle size.

Individual drops of water containing suspended silt particles were applied to the surface of the flowing film of water to simulate the introduction of raindrop-detached material into the overland flow process. Because the quantity of silt involved was small, a Coulter Counter

was employed to perform particle size analysis on the deposited material.

An analysis of particle size versus amount deposited at specific points down slope from the point of introduction revealed a peak deposition distance in each case which decreased with increasing surface roughness. A minimum retention was observed for a particle size of approximately eight microns under all conditions tested. Several velocity profiles were assumed using conventional transport theories in an attempt to mathematically model the phenomena.

Approved

Major Professor

Approved

Department Chairman

SILT TRANSPORT BY THIN FILM FLOW

Ву

Terence Hugh Podmore

A THESIS

Submitted to
Michigan State University
in partial fulfillment of the requirements
for the degree of

MASTER OF SCIENCE

Department of Agricultural Engineering

ACKNOWLEDGMENTS

I wish to extend my sincere thanks to Dr. George E. Merva for his endless patience and guidance during this study. His help and suggestions during the research were especially valuable. It has been a privilege to work with him.

My thanks go to the other members of my committee, Professor Ernest H. Kidder and Professor Earl A. Erickson, for their help and co-operation.

Special appreciation is extended to Professor Theodore

I. Hedrick for the use of the Coulter Counter, and for his
understanding during the course of its use.

I would like to thank my parents, Mr. and Mrs.

Arthur Podmore, for constant encouragement during the whole course of my education. Also, to my parents-in-law, Mr. and Mrs. Carl M. Lipscomb, for raising such a wonderful daughter, and for providing a home-from-home in America.

This thesis is dedicated to my wife, Carol Ann, without whose constant love and sense of humor, this work would have been given up for lost.

TABLE OF CONTENTS

					Page
ACKNOWLEDGMENTS	•	•	•	•	11
LIST OF TABLES	•	•	•	•	v
LIST OF FIGURES	•	•	•	•	vi
LIST OF SYMBOLS	•	•	•	•	viii
INTRODUCTION	•	•	•	•	1
LITERATURE SURVEY	•	•		•	4
RATIONALE AND OBJECTIVES	•	•	•	•	13
EXPERIMENTAL AND THEORETICAL CONSIDERAT	CION	ıs.	•		14
Theoretical Models	•		•	•	14 27 33 35 41
TEST PROCEDURES	•	•	•	c	47
Flow Test Procedure	o c	•		n	47 50
DATA ANALYSIS	٥	•	•	3	54
DISCUSSION OF RESULTS	٠	•	o	c	71
SUMMARY AND CONCLUSIONS	٠	¢	c	٠	80
Summary	•	•		•	80 81
RECOMMENDATIONS	•	•	•	۰	82
Further Improvements on the Present Recommendations for Further Study.	: St	udy	•	٠	82 83

														Page
REFERENCES.	•	•	•	•	•	•	•	•	•	•	•	•	•	85
APPENDICES,	•	•	•	•	•	•	•	•	•	•	•	•	•	89
Appendix	Α.													
A	Б												•	90
Appendix	в.					-	_	•	of .			-		7.00
	•								•					100
Appendix	C.	D	ata	•	•	•			•	•	•		•	103

LIST OF TABLES

Table		Page
1.	Slope Data from Site 1	28
2.	Slope Data from Site 2	30
3.	Comparison of Degree of Detachability and Transportability	33
4.	Sample Coulter Counter Data	52
5.	Analysis of Data of Table 4	53

LIST OF FIGURES

Figure		Page
1.	Diagram of flow conditions	17
2.	Photograph of Site 1	29
3.	Photograph of Site 2	31
4.	Graph of velocity of flow	38
5.	Photograph of equipment	39
6.	Diagram of apparatus used to produce thin film flow	40
7.	Graph of typical flow profile	42
8.	Photograph of Coulter Counter	46
9.	Typical deposition curve	57
10.	Graphs of theoretical models	58
11.	Comparison of two tests (40-grade)	59
12.	Comparison of two tests (80-grade)	60
13.	Comparison of two tests (glass bed)	61
14.	Comparison of runs (1% slope, low flow)	62
15.	Comparison of runs (1% slope, medium flow).	63
16.	Comparison of runs (3% slope, low flow)	64
17.	Comparison of runs (3% slope, medium flow).	65
18.	Comparison of runs (5% slope, low flow)	66
19.	Comparison of runs (5% slope, medium flow).	67
20.	Comparison of slopes (glass bed and low flow)	68

Figure		Page
21.	Comparison of slopes (80-grade bed and low flow)	69
22,	Comparison of slopes (40-grade bed and low flow)	70
23.	Graph of total particle retention (glass bed)	76
24.	Graph of total particle retention (80-grade bed)	77
25.	Graph of total particle retention (40-grade bed)	78
26.	Diagram of Coulter Counter	92

LIST OF SYMBOLS

```
Amplification
Α
A *
       Constant
       Constant
В
       Constant
C
C<sub>T.</sub>
      Lift Coefficient
C_{r}
       Coefficient of Resistance
d
       Density of water
       Equivalent spherical diameter (cm.)
d<sub>T</sub>
       Density of Silt (gm./cm.^3)
d_{s}
\overline{d}
       Particle diameter (cm.)
       Depth of Flow (cm.)
D
\overline{\mathbb{D}}
       Mean depth of Flow (cm.)
D+
       Dimensionless Film Thickness
f
       Function of
       Acceleration due to gravity (980 cm./sec.<sup>2</sup>)
       Coulter Counter Calibration Constant
       Aperture Current
Ι
k
       Stoke's Law Constant
K
       Constant
       as subscript, Maximum
max
       Full particle count
nf
       Particle half count
n_{m}
```

```
Particle oversize count
n_{0}
Ρ
      Percentage slope
      Particle radius (cm.)
R
      Constant
      Time (seconds)
      Threshold value (Coulter Counter)
t<sub>T.</sub>
      Flow velocity in x-direction (cm./sec.)
u
11
      Mean Flow Velocity (cm./sec.)
      Surface velocity (cm./sec.)
u
u+
      Dimensionless velocity
u*
      Friction velocity (cm./sec.)
      Velocity (cm./sec.)
V
      Volume of particle (cm.^3)
v_{T}
      Terminal velocity of silt (cm./sec.)
V _
      Component of v_s in x-direction (cm./sec.)
<sup>V</sup>sx
      Component of v_s in y-direction (cm./sec.)
<sup>V</sup>sy
      Critical Threshold Velocity (ft./sec.)
V+
      Distance along axial coordinate (cm.)
Х
       (Where i = integer) Particle count
X;
\bar{x}
      Mean particle count
X
      Critical Distance (cm.)
      Distance along vertical coordinate (cm.)
У
      Shear stress (gm./cm. sec.<sup>2</sup>)
τ
      Kinematic Viscosity (cm. 2/sec.)
      Viscosity (gm./sm. sec.)
μ
```

θ

Angle (Degrees)

INTRODUCTION

The author became interested in soil erosion while working for his Bachelor's degree. A study of the literature available showed a gap in information related to the erosion process. Ellison (1947), Meyer (1958, 1965), Rose (1960), and Hudson (1963) have investigated the splash erosion process. The transport of eroded material by streams and rivers has had special attention from Einstein (1964), Kalinske (1947), and various other workers.

Conventional concepts of erosion have suggested that the process begins with the detachment of soil particles caused by the splash impact of falling raindrops. The detachment is followed by sheet erosion in which the detached material is removed by rainfall running off the watershed in the form of a uniform sheet. Although the latter concept has had considerable acceptance, it has been shown to be incorrect (Schwab et al., 1966). The flow of water as a sheet occurs for only a short distance before forming into micro-rills. The formation of micro-rills is the first stage in the concentration of flowing water. The micro-rills join to form rills which in turn form gullies.

Rill erosion is characterized by the movement of soil material in suspension and by bed drag. Conventionally, rill erosion occurs when the rill is large enough to be well defined and easily seen. Gully erosion is an advanced stage of rill formation where scour of the channel bed occurs due to the excess energy in the flowing water. Gullies are a major hazard to agriculture since they remove soil, create water channels, and continue to enlarge indefinitely unless action is taken.

For a more complete understanding of erosion mechanics it was considered necessary to investigate the interrelationship between splash erosion detachment and transport of eroded material by streams and rivers. The transportation mechanics of the intermediate stage linking these two phases of the erosion process was to be the subject of this study, together with the factors which influence the process.

Following a literature survey, it was decided that a study of the transportation capacities of thin films of flowing water would contribute valuable information concerning the soil erosion process. The runoff process would be simulated to determine its role in the transportation of eroded material from the point of detachment to a stream of water having sufficient velocity to prevent settling out of eroded material.

If a film of flowing water could be simulated and its transportation characteristics determined in the study,

one could then determine the description of the rill constituting an erosion threat since the eroded material must reach water moving with sufficient velocity to maintain its suspension and prevent deposition in the micro-rills as sediment. Thus a critical distance of transport could be found for suspended material in thin film flow.

LITERATURE SURVEY

The literature survey began with the work of W. D. Ellison, an early investigator in the scientific study of soil erosion by water. Ellison (1946) defines soil erosion as "a process of detachment and transportation of soil materials by erosive agents." In his 1947 publication he amplifies the definition as follows:

This definition describes the erosion process as consisting of two principal sequential events. In the first event soil particles are torn loose (detached) from their moorings in the soil mass and made available for transport. In the second event, detached soil materials are transported. We cannot combine these two processes and express them as a single quantitive result, because they cannot be expressed in like units.

Ellison (1947) indicates that the erosive capacity of an eroding agent is divided into (a) a detaching capacity and (b) a transporting capacity. In this study only the transporting capacity is considered. Ellison's work on splash erosion was thoroughly reviewed in six articles in Agricultural Engineering (1947). Widespread investigation into the erosive nature of rainfall and water drop splash subsequently took place.

Hudson (1964) reviewed the development of rainfall simulators including thread droppers, nozzle droppers, and spray simulators. Of these the spray simulator has been

given the most attention. One of the most successful devices is the Rainfall Simulator which was developed by Meyer (1958). The Rainfall Simulator has almost become a standard for soil and water loss evaluations.

Using a rainfall simulator similar to that of Meyer, Rose (1960) investigated some aspects of soil detachment including the relationships between rate of soil detachment, rainfall momentum, and rainfall kinetic energy.

Palmer (1965) measured the force of water drop impact under varying conditions and Mutchler (1967) investigated the parameters for describing raindrop splash.

The above works have been cited to indicate the extent of investigation revealing the present state of knowledge concerning splash erosion. However, Ellison (1947) makes it clear that both detachment and transportation must occur in sequence before significant erosion results. Detachment under rainfall action alone merely produces soil movement in random directions in a restricted area with no net soil loss.

The problem of soil particle transportation by water has been largely investigated by civil engineers dealing with "sediment load" in rivers and streams. In the literature on this subject, the suspended material is referred to as "sediment." However, according to Webster's Seventh New Collegiate Dictionary (1961 Edition) "sediment" is defined as: "The matter that settles to the bottom of

a liquid." Thus, the use of the term "sediment load" and other related terms is incorrect. A more appropriate description would be "suspended material load" or, in the context of soil erosion, "eroded material load." These terms will be used when applicable. Sediment transportation, which has widespread use in present literature, is more accurately described as "the transport of suspended, eroded material." Whether or not this material becomes sediment is the subject of this research.

The investigators of suspended material transportation are concerned with the prevention of channel erosion or silting. To avoid silting a minimum velocity approach is used. Chow (1959) outlines this approach for nonerodible channels where the maximum permissible velocity—that is, the maximum velocity which will not cause erosion—can be ignored. Chow (1959) states that minimum permissible velocities for given suspended particle diameters are very uncertain. He adds that a mean velocity of 2 to 3 feet per second can be used safely in most cases when the percentage of silt present in the channel is small. For erodible channels a maximum permissible velocity is used since scour of the channel will occur. Values of water velocity for channels of varying compositions are given.

The process of suspended material movement in channels is outlined by Schwab, et al. (1966):

Sediment in streams is transported by suspension, by saltation, and by bed load movement. Although many theoretical and empirical relationships have been developed between the suspended material transport capacity of the stream, it is not possible to predict suspended material loads with any degree of accuracy. . . .

... Variables affecting suspended material movement include velocity of flow, turbulence, size distribution, diameter, cohesiveness, and specific gravity of transported materials, channel roughness, obstructions to flow, and the availability of materials for movement.

The suspended material fraction is defined by Schwab, et al. (1966) as that material which remains in suspension in flowing water for a considerable period of time without contact with the stream bed.

The phenomenon of "saltation" mentioned previously is most commonly associated with movement of soil particles in air. However, it is also present in stream transport of eroded material according to Schwab, et al. (1966). He states:

Sediment movement by saltation occurs where the particles skip or bounce along the stream bed. The height of the bounce, expressed in mathematical form, is directly proportional to the ratio of particle density to fluid density. Particles in water rise only a few particle diameters for most practical conditions. In comparison to total suspended material transported saltation is considered relatively unimportant.

Einstein (1964) describes saltation in a similar manner, but adds:

Saltation of the kind taking place in the air is impossible in water, as Kalinske (1942) has shown very convincingly. . . . Saltation is unimportant as a separate mode of particle motion in water, but may be a part of the bed-load movement, where the rolling and sliding particles sometimes jump at small distances.

Bed-load is defined (Schwab, et al., 1966; Einstein, 1964, pp. 17-37; and Raudkivi, 1967, p. 45) as suspended material that moves in almost continuous contact with the stream bed, being rolled or pushed along the bottom by the force of the water. Bed load is generally considered to be one of the major factors of suspended material movement in streams.

Bed load is difficult to determine experimentally and empirical formulae have been developed to express it. None of the many empirical formulae developed to give the rate of the bed load movement have been entirely satisfactory. Laboratory studies (Mavis, 1935) have shown that the critical threshold velocity required to initiate movement of particles in the bottom of a stream is expressed by an empirical equation of the form,

$$v_{t} = \frac{1}{10} r (d_{s} - d)^{\frac{1}{2}}$$

where

 v_t = threshold velocity (ft./sec.)

r = particle radius (cm.)

 $d_s = density of silt particles (gm./cm.³)$

d = density of water $(gm./cm.^3)$

(This is limited to unigranular materials ranging in diameter from 0.35 to 5.7 mm. and in specific gravity from 1.83 to 2.64).

Einstein (1964) gives an excellent account of the present state of sedimentation. He defines his concept of "Dual Control of Sediment Transport":

Every sediment particle which passes a particular cross section of the stream must satisfy two conditions: 1.) It must have been eroded from somewhere in the watershed above the cross section; 2.) It must be transported by the flow from the place of erosion to the cross section.

Each of these two conditions may limit the sediment rate at the cross section, depending on the relative magnitude of the two controls; the availability of the material in the watershed; and the transporting ability of the stream. In most streams the finer part of the load, i.e. the part which the flow can easily carry in large quantities, is limited by its availability in the watershed. This part of the load is designated as the 'wash load.' The coarser part of the load, i.e. the part which is more difficult to move by flowing water, is limited in its rate by the transporting ability of the flow between the source and the section. This part of the load is designated as 'bed-material lead.'

Einstein (1964) also indicates the effect of particle settling velocity:

When a sediment grain moves through water, it experiences considerable resistence which is a function of the Reynolds number of this movement. When the particle moves downward, a settling velocity will be reached at which the resistence equals the weight of the grain in water.

For laminar and turbulent flow, the settling velocities for spherical grains have been shown to be as follows:

Laminar flow
$$v_s = \frac{2}{9} \frac{(d_s - d)}{\mu} gr^2$$

Turbulent flow
$$v_s = \sqrt{(d_s - d) \frac{8}{3} \frac{gr}{C_r}}$$

Where

 v_s = settling velocity, cm./sec.

 $d_s = density of silt, gm./cm.^3$

 $d = density of water, gm./cm.^3$

r = particle radius, cm.

g = acceleration due to gravity, cr 980 cm/sec.²

 μ = viscosity of fluid, gm./cm. sec.

Cr = coefficient of resistence, depending on Reynolds number, with a value of about 0.5 for a large range of Reynolds numbers above critical.

Einstein (1964) further outlines a procedure for determining the suspended material load as a function of the bed load composition and the flow. This is not applicable for the present work since it does not take account of the effects of the boundary layer. A thorough analysis of laminar and turbulent boundary layer theory is given by Schlichting (1968). Reference will be made to this topic in the theoretical considerations.

The most recent comprehensive work available on suspended material transport is the publication of Raudkivi (1967). Here most of the various formulae in use are compared and contrasted. Work on threshold of particle transport is also discussed. This has been very useful for this study and will be dealt with in greater detail later.

The literature reviewed gave an indication of the present state of knowledge on the two most researched

aspects of erosion; detachment by water drop impact, and transport phenomena in large water masses. The conventional theories of suspended material transportation consider much greater depths and quantities of flowing water as opposed to the thin films used in this approach. Hence these theories were considered to be largely inapplicable, although note was taken of the methods used.

An account of the theory and practice in the description of thin film flow has been compiled by Fulford (1964). He discusses laminar and turbulent flow together with interactions of the liquid with the walls of the channel and the surrounding fluid. The effect of boundary layers is discussed. The latter effect is considered to void the theories of suspended material transportation at present in use for streams and rivers as applied to thin film flow. Fulford (1964) cites the "universal velocity equations" of Nikuradse (1942) which will be introduced and used later.

Fulford (1964) also presents an analysis of the Navier-Stokes equations for smooth, laminar, two-dimensional film flow which describes the velocity distribution in terms of a semi-parabolic equation.

$$u = \frac{g}{v} (\sin \theta) (Dy - \frac{y^2}{2})$$

where the surface velocity is

$$u_s = \frac{gD}{2v} \sin \theta$$

and the mean velocity is

$$\overline{u} = \frac{gD}{3v}$$
 sin θ

hence,

$$u_s = 1.5\overline{u}$$

A full theoretical analysis applied to the present study is given in a later section.

Meyer and Monke (1965) investigated the mechanics of soil erosion by the combined action of rainfall and overland flow. Commercial glass beds were used to simulate a soil bed, the smallest particle used having a diameter of 58 microns. Rainfall and shallow depths of flowing surface water could be applied simultaneoulsy. Slope steepness, slope length, and particle size were the variables studied.

It was found that runoff erosion increased rapidly with increasing slope steepness and length. Smaller particle sizes were more erosive at most slope steepness and lengths, but the larger sizes were more erosive at small steepness and lengths. Rainfall plus runoff, as compared with runoff alone, increased the erosion of the smaller particle sizes but decreased the erosion of the larger sizes. The study was among the first to simulate the process of soil erosion as a whole in the laboratory.

RATIONALE AND OBJECTIVES

The literature survey has indicated an area of deficient information concerning the erosion process, that is, the mechanics of eroded material transportation from the point of detachment to water moving with sufficient velocity to maintain the eroded particles in suspension. In an effort to contribute information to this area the study reported on in this thesis has as its objective to investigate the variables which may affect the transport of eroded material by thin film flow.

These variables were assumed to be:

- 1. Degree of slope
- 2. Flow rate
- 3. Surface roughness
- 4. Length of slope
- 5. Particle size.

The first step was to formulate a mathematical model of the flow conditions. The second step was the investigation of the variables given above to attempt to establish their effect on the transport. The final step was to determine the validity of the mathematical models.

EXPERIMENTAL AND THEORETICAL CONSIDERATIONS

Theoretical Models

Stoke's law of settling is used in this study. Baver (1956) states Stoke's law as follows:

$$v_s = \frac{2}{9} \frac{(d_s - d)}{u} gr^2$$

and gives the assumptions necessary for this formula to apply. These are:

- 1. The particles must be large in comparison to liquid molecules so that Brownian movement will not affect the fall. This is true for all soil particles except colloidal clays (Baver, 1956, p. 17).
- 2. The extent of the liquid must be great in comparison with the size of the particles. The fall of the particles must not be affected by the proximity of the wall of the vessel or adjacent particles. This condition was considered when the experiment reported on in this thesis was designed.

- 3. The particles must be rigid and smooth. This condition is difficult to fulfill with soil particles. It is highly probable that the particles are not completely smooth over their entire surface. It is fairly well established that the particles are not spherical but are irregularly shaped with a large number of plateshaped particles present in the clay fractions. Since variously shaped particles fall with different velocities, the term "equivalent or effective radius" is used to overcome this difficulty in Stoke's law. "Equivalent or effective radius" is defined as the radius of a sphere of the same material which would fall with the same velocity as the particle in question.
- 4. There must be no slipping between the particles and the liquid. This requirement is easily fulfilled in the case of soils because of the water hull around the particles.
- 5. The velocity of fall must not exceed a certain critical value so that the viscosity of the liquid remains the only resistance to the fall of the particle. Particles larger than silt cannot be separated accurately by Stoke's law.

From the above considerations:

- a. Colloidal clays are excluded because of effects due to Brownian movement.
- b. The clay fraction is excluded due to the platelike nature of the particles.
- c. The sand fraction cannot be separated by Stoke's Law.

Therefore the silt fraction was considered to conform to the predictions of Stoke's law. Further reasons for choosing the silt fraction are given later.

Stoke's law is used with all velocity profile models to give expressions for distance of particle transport. The procedure used is given as follows:

The velocity profile model is of the form

$$u = f(y)$$

The velocity of the particle is given from Stoke's Law as

$$v_s = \frac{2}{9} \frac{(d_s - d)}{u} gr^2$$

and for a given set of conditions

$$v_s = kr^2$$

The reference frame used is shown in Figure 1. Consider the vertical velocity from Stoke's Law in the x-y frame of reference.

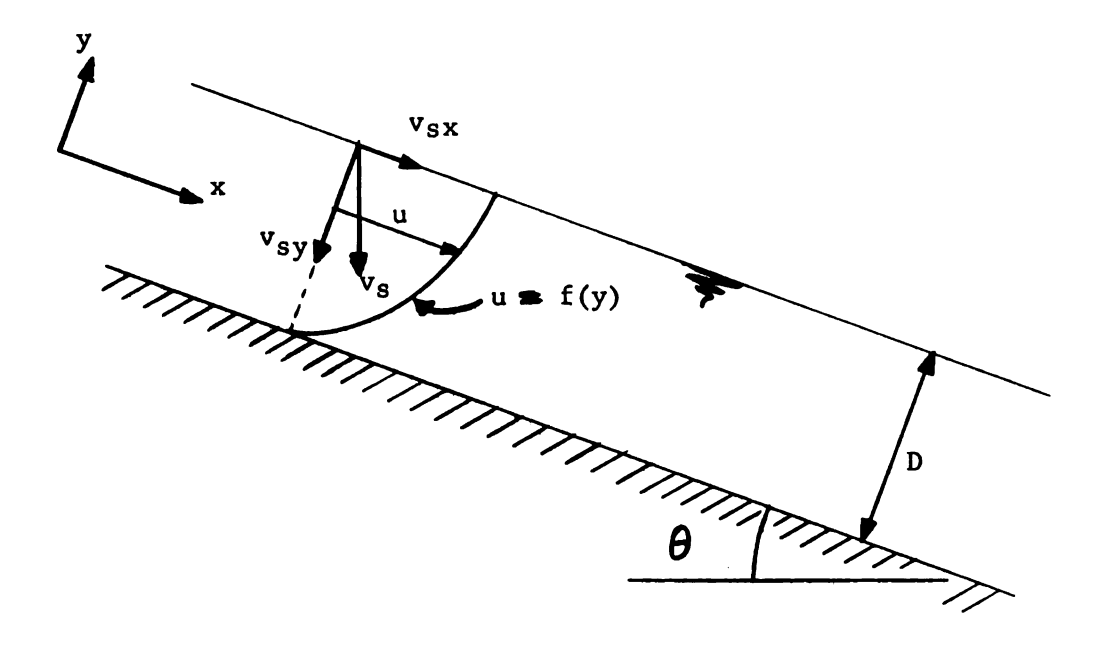


Figure 1. Diagram of flow conditions used in theoretical analysis. Note coordinate system used. Velocity profile is some function of depth.

One has

$$v_{sx} = + v_{s} \sin \theta$$

$$v_{sy} = -v_{s} \cos \theta$$

and for small angles: $(\theta \le 5^{\circ})$

$$v_{sx} = Pv_{s} = Pkr^{2}$$

$$v_{sy} = -v_s = -kr^2$$

where $\theta = P = percentage slope$.

Since the particle is moving in water, perfect coupling is assumed. This is similar to Assumption 4 for Stoke's Law and is justified by the same statement (Baver, 1956, p. 56).

To find the components of velocity of the particle in the x-y frame note that in the x-direction the velocity is

$$u = Pkr^2 + f(y) \tag{1}$$

Where

Pkr² = component due to effects of gravity
on particle

f(y) = component due to the effects of fluid velocity.

In the y-direction one has

$$v = kr^2$$

The velocity components thus obtained can be utilized to determine a Critical Distance for particle deposition as follows:

$$v = \frac{dy}{dt} = - kr^2$$

and integrating from D to some depth y one obtains;

$$y - D = -kr^{2}t$$

$$y = D - kr^{2}t$$
(2)

when

$$t = t_{max} y = 0$$

therefore

$$t_{max} = \frac{D}{kr^2}$$

Using equation (1) one can write

$$u = \frac{dx}{dt} = Pkr^2 + f(y)$$
 (3)

and by making use of equation (2) one can obtain, with equation (3)

$$\frac{dx}{dt} = Pkr^2 + f(D - kr^2t)$$
 (4)

Equation (4) can be integrated to obtain

$$x = Pkr^{2}t + \int_{0}^{t} f(D - kr^{2}t)dt$$

When x = X (Critical Distance)

$$t = t_{\text{max}} = \frac{D}{kr^2}$$

therefore

$$X = PD + \int_{0}^{D/kr^{2}} f(D - kr^{2}t)dt$$
 (5)

In the experiments reported on in this study

$$P_{\text{max}} \leq 5^{\circ} \leq 0.05$$

and

$$D_{\text{max}} = 0.284 \text{ cm}.$$

The maximum value of the product PD is 0.05 x 0.284 or 1.42×10^{-3} cm. Hence the PD term can be ignored. Therefore the general expression for X is

$$X = \int_{0}^{D/kr^{2}} f(D - kr^{2}t)dt$$
 (6)

It can be seen that from the above equation that the Critical Distance X is only dependent on the depth D and those factors influencing the Stoke's Law settling when they are introduced by the velocity profile function f(y).

The veolicty profiles considered in this study were:

1. A velocity constant with depth with a sharp reduction to zero velocity close to the bed surface. This model approximates to the turbulent condition.

$$f_1(y) = constant = \overline{u}$$

Therefore

$$x_1 = \overline{u} \int_{0}^{D/kr^2} dt = \overline{u} \frac{D}{kr^2}$$
 (7)

2. A first order relationship between velocity and depth, as proposed by Newton for laminar flow ignoring boundary layer effects.

$$\tau = \mu \frac{du}{dy}$$

or

$$f_2(y) = \frac{u_s y}{D} = \frac{2\overline{u}y}{D}$$

Therefore

$$X_2 = \frac{2\overline{u}}{D} \int_0^{D/kr^2} (D-kr^2t) dt = \overline{u} \frac{D}{kr^2}$$
 (8)

3. A second order relation between velocity and depth from the solution of the Navier-Stokes equations for smooth, laminar, two-dimensional film flow (Fulford, 1964, p. 156).

$$f_3(y) = \frac{g}{v} \sin \theta (Dy - \frac{y^2}{2}) = \frac{gP}{v} (Dy - \frac{y^2}{2})$$

and therefore

$$x_3 = \frac{gP}{v} \int_0^{D/kr^2} (Dy - \frac{y^2}{2}) dt = \frac{gPD^3}{3vkr^2}$$
 (9)

4. A second order relation between velocity and depth from consideration of the lift force on a particle just above the bed surface. (See, for instance, Streeter, 1958, p. 171.) By equating this lift force to the gravitational force on the particle one has,

Lift force =
$$\frac{C_L A(d_s - d)u^2}{2}$$
 where $A = \pi r^2$

Gravitational force =
$$\frac{4}{3} \pi r^3 (d_s - d)g$$

and equating these forces to give zero net vertical force,

$$u^2 = \frac{8rg}{3C_{T_i}} \tag{10}$$

Equation (10) is assumed valid for r in the range 2.5 to 25 microns, the range of particle radii used in the study. It is assumed that equation (10) applies to the whole film thickness. Thus

$$f_{\mu}(y) = \sqrt{\frac{8g}{3C_{L}}} y$$

and therefore

$$X_{4} = \sqrt{\frac{8g}{3C_{L}}} \int_{0}^{D/kr^{2}} (D-kr^{2}t)^{\frac{1}{2}} dt = \sqrt{\frac{8g}{3C_{L}}} \frac{2D}{3kr^{2}}$$
 (11)

depth was considered so that account could be taken of special conditions suggested by the experimental results. The general equation considered has the form:

$$y = R + A*u + Bu^2 + Cu^3$$
 (12)

Where R, A^* , B, and C are constants. To evaluate these constants boundary conditions must be supplied. The primary boundary condition requires that when y = 0, u = 0 then R = 0.

The general equation becomes with the above conditions

$$y = A*u + Bu^2 + Cu^3$$

The remaining three boundary conditions necessary are evaluated for specific cases. Equation (12) requires that one use a different approach to find X. Note,

$$u = \frac{dx}{dt} = \frac{dx}{dy} \quad \frac{dy}{dt} = \frac{dx}{dy} \quad v = -kr^2 \quad \frac{dx}{dy}$$
so that
$$-kr^2 \quad dx = u \quad dy$$

if one uses equation (12)

$$dy = (A* + 2Bu + 3Cu^2)du$$

After integrating one obtains

$$-kr^{2}[x]_{0}^{X} = \int_{u_{s}}^{0} u(A^{*} + 2Bu + 3Cu^{3})du$$

$$X_{5} = \frac{1}{kr^{2}} \left[\frac{A*u_{s}^{2}}{2} + \frac{2Bu_{s}^{3}}{3} + \frac{3Cu_{s}^{4}}{4} \right]$$
 (13)

6. A discontinuous velocity profile utilizing the "universal velocity profile equations" of Nikuradse (1942) given by Fulford (1964, p. 171).

$$u^{+} = y^{+}$$
 for $0 \le y^{+} \le 5$ (laminar sub-layer)
 $u^{+} = -3.05 + 5.0 \text{ ln } y^{+}$ for $5 \le y^{+} \le 30$ (buffer layer)
 $u^{+} = 5.5 + 2.5 \text{ ln } y^{+}$ for $30 \le y^{+} \le D^{+}$ (turbulent zone)

where

$$u^+ = \frac{u}{u^*}$$
 (dimensionless velocity)

$$y^+ = y \frac{u^*}{v}$$
 (dimensionless distance from wall)

$$D^{+} = D\frac{u^{*}}{v}$$
 (dimensionless film thickness)

$$u^* = \left(\frac{\tau}{d}\right)^{\frac{1}{2}}$$
 (friction velocity)

and

$$τ = Ddg sin θ$$
 (shear stress)

In the laminar sub-layer,

$$\frac{D}{kr^2} \ge t > \left(D - \frac{5v}{(Dg P)^{\frac{1}{2}}}\right) \frac{1}{kr^2}$$

$$u = \frac{DgP}{v} y \tag{14}$$

In the buffer layer,

$$\frac{1}{kr^{2}} \left(D - \frac{5v}{(Dg P)^{\frac{1}{2}}} \right) \stackrel{>}{=} t > \frac{1}{kr^{2}} \left(D - \frac{30v}{(Dg P)^{\frac{1}{2}}} \right)$$

$$u = (DgP)^{\frac{1}{2}} (-3.05 + 5.0 l_n (\frac{y(DgP)^{\frac{1}{2}}}{v}))$$
 (15)

In the turbulent zone,

$$\frac{1}{kr^2} \left(D - \frac{30v}{(DgP)^{\frac{1}{2}}} \right) \ge t \ge 0$$

$$u = (DgP)^{\frac{1}{2}} (5.5 + 2.5 l_n (\frac{y(DgP)^{\frac{1}{2}}}{v}))$$
 (16)

And using equations (14), (15) and (16) in equation (6) the general expression for the Critical Distance is:

$$X_{6} = \int_{\frac{1}{kr^{2}}(D - \frac{30v}{(DgP)^{\frac{1}{2}}})}^{0} (5.5 + 2.5 \, l_{n}(\frac{(D - kr^{2}t)(DgP)^{\frac{1}{2}}}{v})dt$$

$$+ \int \frac{\frac{1}{kr^{2}}(D - \frac{30v}{(DgP)^{\frac{1}{2}}})}{(DgP)^{\frac{1}{2}}(-3.05 + 5.0 l_{n}(\frac{(D - kr^{2}t)(DgP)^{\frac{1}{2}}}{v})dt}$$

$$+ \int \frac{1}{kr^{2}}(D - \frac{5v}{(DgP)^{\frac{1}{2}}})$$

$$+ \int \frac{\frac{1}{kr^{2}} (D - \frac{5v}{(DgP)^{\frac{1}{2}}})}{\frac{DgP}{v} (D - kr^{2}t)dt}$$
(17)

From the above expressions for X, it can be seen that they all take the form:

$$X = \frac{K}{kr^2} \tag{18}$$

Therefore, from given initial conditions it ought to be possible to predict values of the critical distance X for given particle diameters using the appropriate form for f(y).

Initial Considerations

Before the experiment was begun, a preliminary study was carried out to determine the range of slopes frequently found on a natural watershed. Open ground was chosen and obvious rills and gullies were avoided. The maximum slopes were measured in every case, since this would be the path taken by flowing water. The distances measured in each case were of the order of 10 cm. and the slopes were determined using a piece of apparatus consisting of a level and a 60 cm. straight-edge fastened together in parallel and used in conjunction with a hand held vertical scale. The level was held horizontal with one end of the straight-edge touching the soil surface. The distance between the straight-edge and the soil surface was measured at various points with the vertical scale.

each case and the slopes were calculated. This process was carried out at two separate sites, which are described below. Approximately 50 slopes were measured on each site.

Site 1

This site was situated on the west side of Lansing, Michigan, near the Grand River. It was a development site from which most of the surface vegetation had been removed. Vegetation had begun to return, but a large proportion of the soil surface remained bare. The type of soil was predominantly sand, and measurements were taken on locations such as that shown in Figure 2(a). Stones and gravel can be seen exposed by erosion of the surrounding material. Considerable erosion had taken place on parts of the site due to concentration of surface runoff as can be seen in Figure 2(b). The level shown in the figures is 60 cm. long giving a scale to the figures. Results of the slope analysis are given in Table 1.

Table 1. Data from Site I

Slope (%)	No. of Slopes	Mean Slope Length (cm.) (±0.5)
< 2.50	0	
2.50 - 7.49	9	22.6
7.50 - 12.49	31	20.5
12.50 -17.49	7	17.4
>17.50	- 2	19.7





Figure 2. Photographs of Site 1.

Above: (a) Area on which measurements were taken.

Below: (b) Gully erosion on Site 1.

(Scale shown is 60 cm. long.)

Site 2

This site was also situated on the west side of Lansing and it had been cleared for development. As can be seen from Figures 3(a) and 3(b), considerable runoff has taken place and gully erosion is beginning. The type of soil is a clay loam subsoil, which has been exposed by scalping the topscil. There was little trace of organic matter in the soil. This was considered to give the worst erosion conditions for this type of soil. Again the level is used for a scale (60 cm.). Exposed stones and gravel can be seen on the surface. When examined, the soil was dry and cracking had occurred. Results of the slope analysis are given in Table 2.

Table 2. Data from Site 2.

Slope (%)	No. of Slopes	Mean Slope Length (cm.) (±0.5)
< 2.50	11	20.8
2.50 - 7.49	35	15.9
7.50 - 12.49	2	9.5
>12.50	0	
	48	

These two types of soil were considered to give the extremes of the soil composition spectrum. Also, the erosion conditions varied from just beginning on Site 2 to advanced gully formation on Site 1. From the results





Figure 3. Photographs of Site 2.
Above: Area on which measurements were taken.
Below: State of rill erosion on Site 2.
(Scale shown is 60 cm. long.)

obtained it can be seen that the slopes most frequently occurring are in the range of from 0 - 12.49 per cent. These results were used as a guideline in designing the experimental setup for this study.

The mean length of slope is given as an indication of the length expected for a particular slope found in natural conditions and was used in the design of the experimental apparatus. It can be seen from the data in Tables 1 and 2 that the steeper the slope, the shorter the mean slope length. It was indicated therefore that a steep slope produces a more unstable condition, i.e., a short uniform slope is due to more rapid erosion.

To ensure that the experimental conditions correspond to those found during runoff on a watershed, it was necessary to find an indication of depth of flow of runoff. An impermeable bed was to be used in these experiments to eliminate infiltration effects. However, most researchers give their runoff data as a volume flow rate per unit channel width—without indicating values for velocity and depth of flow. The only precise measurements found were those of Osborn (1955), who states:

The normal depths attained by sheet flow under normal field conditions are usually very shallow. Measurement of sheet runoff at rates of 1.25 to 3.68 inches per hour on bare plots up to 20% slope and 116.7 feet length showed depths of flow ranging from 0.06 to 0.15 inches (0.15 to 0.38 cm.).

Since this was the only information of this nature available, it was used as an experimental guideline.

Choice of Eroded Material

Ellison (1947) considered the detachability and transportability of soils. He classified the susceptability of types of soil to detachment and transport in order of highest to lowest as given in Table 3.

Table 3. Comparison of Detachability and Transportability.

Degree	Detachability	<u>Transportability</u>
Highest	Fine sand	Clay
Medium	Silt loam	Silt loam
Lowest	Clay	Fine sand

It can be seen that fine sand is most easily detached and yet least easily transported. The converse is true for clay, while silt loam falls into the middle category in both cases. This indicated that the silt fraction might be the most commonly eroded fraction of the soil medium. Ellison (1947) quotes figures from rainfall studies on aggregation breakdown and runoff when shows that in the runoff for a particular series of tests approximately 87 per cent of the soil material in the surface runoff had a diameter of less than 0.105 mm. (that is, 105 microns) while the original material contained only 53.5 per cent with a diameter of 0.105 mm. or less.

According to the U. S. Bureau of Soils Systems (Baver, 1956, p. 16) silt particles are those in the range 0.05 to 0.005 mm. in diameter.

It was considered that the silt fraction was the most suitable to use in this work since it is the fraction which has both a high detachability and a high trans-portability.

The mechanical properties of silt were given by Buckman and Brady (1960) as follows:

In contrast with the plate-like clay, silt particles tend to be irregularly fragmental, diverse in shape, and seldom smooth or flat. In fact, they are really micro-sand particles, quartz being the dominant mineral. The silt separate possesses some plasticity, cohesion, and adsorption due to an adhering film of clay, but, of course, to a much lesser degree than the clay separate itself.

This similarity of finely crushed sand was further confirmed when the mechanical properties of non-plastic silt was examined and found to conform closely to those of fine to medium sand in properties such as angle of repose and friction angles as given by Hough (1957):

	Slope at angle	Friction angles at		
	of repose	Ultimate Strength	Peak Strength	
Non-plastic Silt	26° - 30°	26° - 30°	30° - 34°	
Uniform fine to medium sand	26° – 30°	26° - 30°	32° - 36°	

Soil containing an appreciable quantity of silt was obtained from a location on the Michigan State University farm. The soil was dried and coarse-sieved to remove organic matter and stones. It was further dried after the large soil aggregates had been broken up manually.

The silt and clay fractions were separated by seiving on a mechanical agitator for five minutes. The fraction passing the finest sieve which was a #300 mesh (62.5 micron apertures) was collected. To remove the silt from the clay, the sample was dispersed with 100 ml. of Calgon solution (containing sodium hexametaphosphate) for 15 minutes in a mechanical mixer. The mixture was then diluted to approximately 1000 ml. with distilled water and placed in a constant temperature bath at 27° C for 30 minutes. The mixture was then thoroughly stirred and left to stand for twe hours.

Most of the liquid was then carefully poured off and the remaining sediment was washed into a dish and evaporated to dryness. This fraction, whose size range was 5 to 50 microns was used in the experiments in the form of a suspension in distilled water. A particle size analysis of the suspension was performed for each run.

Design of Equipment

The equipment was designed to produce conditions of uniform flow. To achieve uniform flow the water supply from the water-main was led into a reservoir. The water

supply was always in excess of the flow rate so that a constant head of water was produced. The water overflowing the reservoir was led to a drain. In this way water-main pressure fluctuation was eliminated. The head difference of water levels was kept constant for all experimental trials.

Two siphons having internal diameters of 0.95 cm. and 1.27 cm. were used to supply low and medium flow conditions. The low flow siphon produced a mean velocity of 16 cm./sec. and a mean flow depth of 0.11 cm. on a smooth bed at 5% slope. The medium flow siphon produced a mean velocity of 23 cm./sec. and a mean flow depth of 0.14 cm. under the same conditions. The siphons were 80 cm. long and made of clear plastic so that the presence of air bubbles could be monitored visually. In preliminary testing it was noted that small air bubbles collected over a period of time on the internal walls of the siphons. This caused an unpredictable change in flow rate. To ensure that this did not occur during testing the flow rate was monitored several times to ensure uniformity and the test completed in about five minutes after the last flow measurement.

The siphon was led to the bottom of the stilling section, a box constructed of plywood having internal dimensions 30 x 30 x 30 cm. for a volume of approximately 0.03 cubic meters of water which was sufficient to damp out most of the turbulence. The assumption was shown to be reasonable by considering the relationship between

velocity and depth for a smooth bed (see Figure 4). The linear relationship indicates smooth laminar flow conditions as predicted by Newton (Streeter, 1958, p. 4).

The stilling section and the flow bed were made in one piece to eliminate sealing problems between the two. The combination was provided with a tilting device to alter the slope of the bed. This was achieved by providing a hinge on the lower edge (see Figure 6). The wedge was calibrated using a level on the bed, and so the bed could be set at any desired inclination. The tilting of the stilling section had negligible effect on the volume or on the head difference in water levels between the stilling section and the reservoir.

The stilling section was provided with a rapid emptying device, which consisted of an inverted U-shaped siphon having an internal diameter of 3.8 cm. In operation this was filled with water and one end placed below water-level in the stilling section. With the water supply removed the remaining water on the bed drained away.

The bed down which the water flowed consisted of a plywood channel 30 cm. wide and 4 cm. deep. The sides of the channel were topped by rails of 1.25 x 1.25 cm. angle section to provide support for the depth measuring device. Fulford (1964, p. 177) gives a review of measuring techniques for mean film thickness. The first and most simple method consists of direct determination of the position of

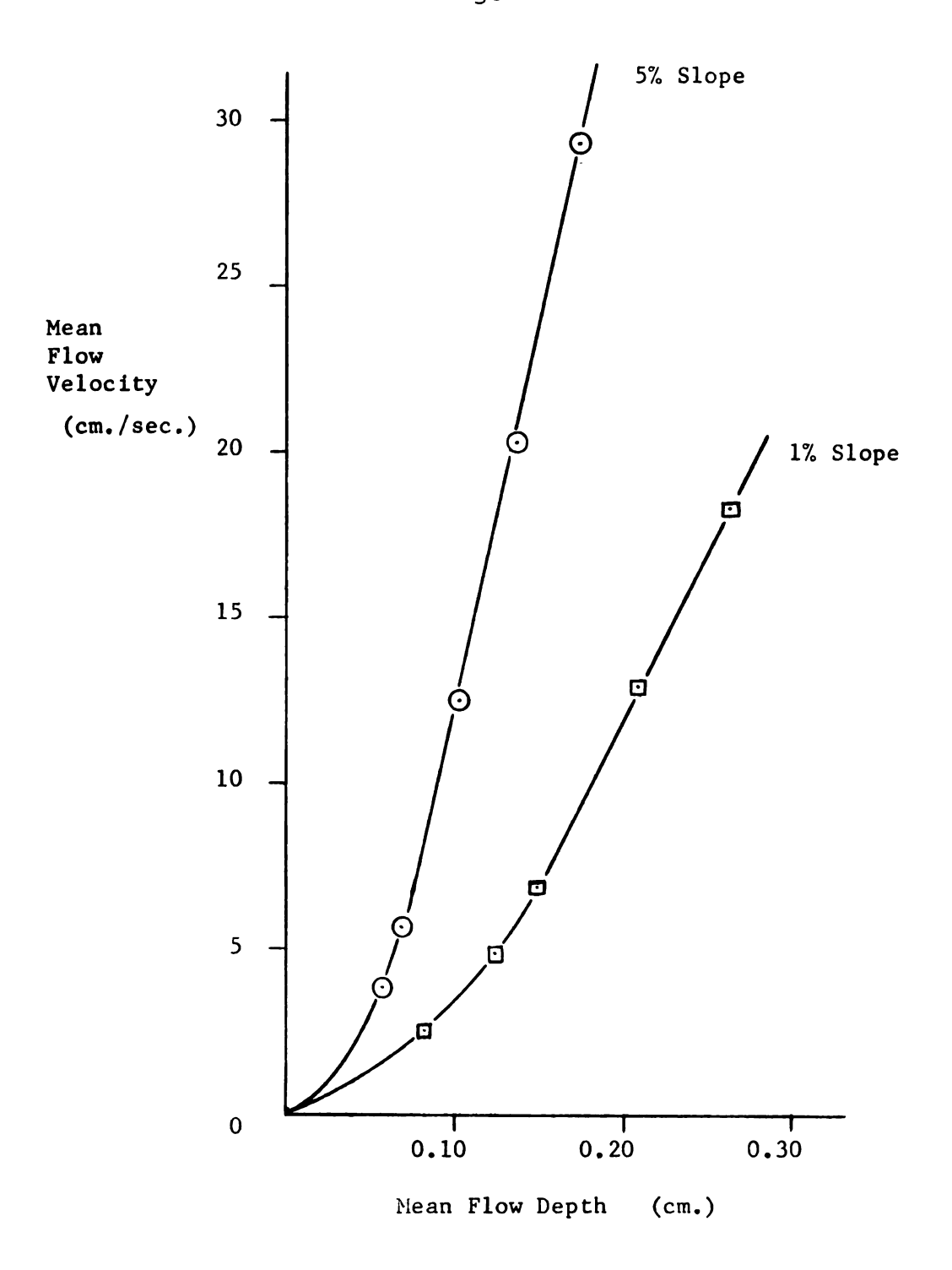


Figure 4. Graph of velocity of flow against depth of flow for a glass plate. The linear portion of the curve indicates laminar flow .

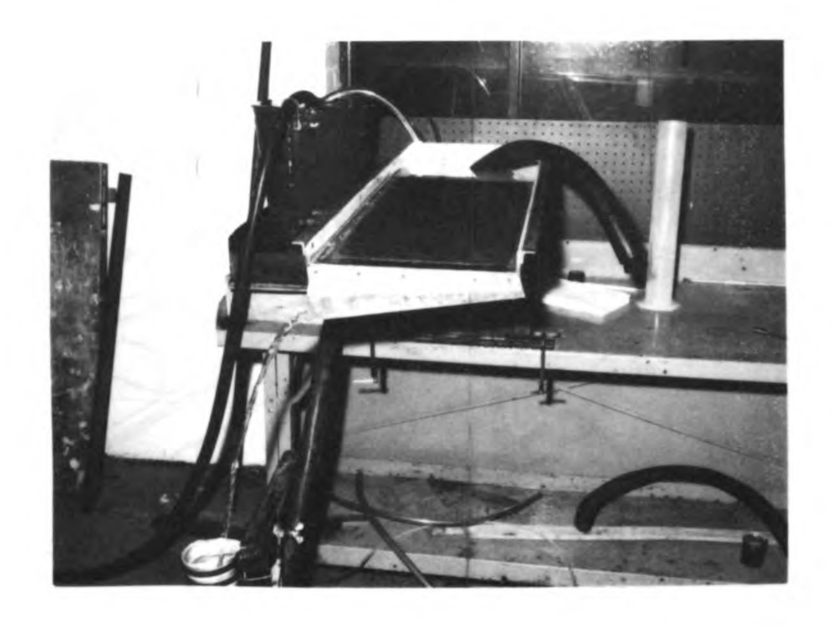




Figure 5. Photographs of experimental stage of study.
Above: (a) General view of apparatus used in the study.
Below: (b) Removal of sample from bed plate. Note
position of squegee and use of wash-bottle.

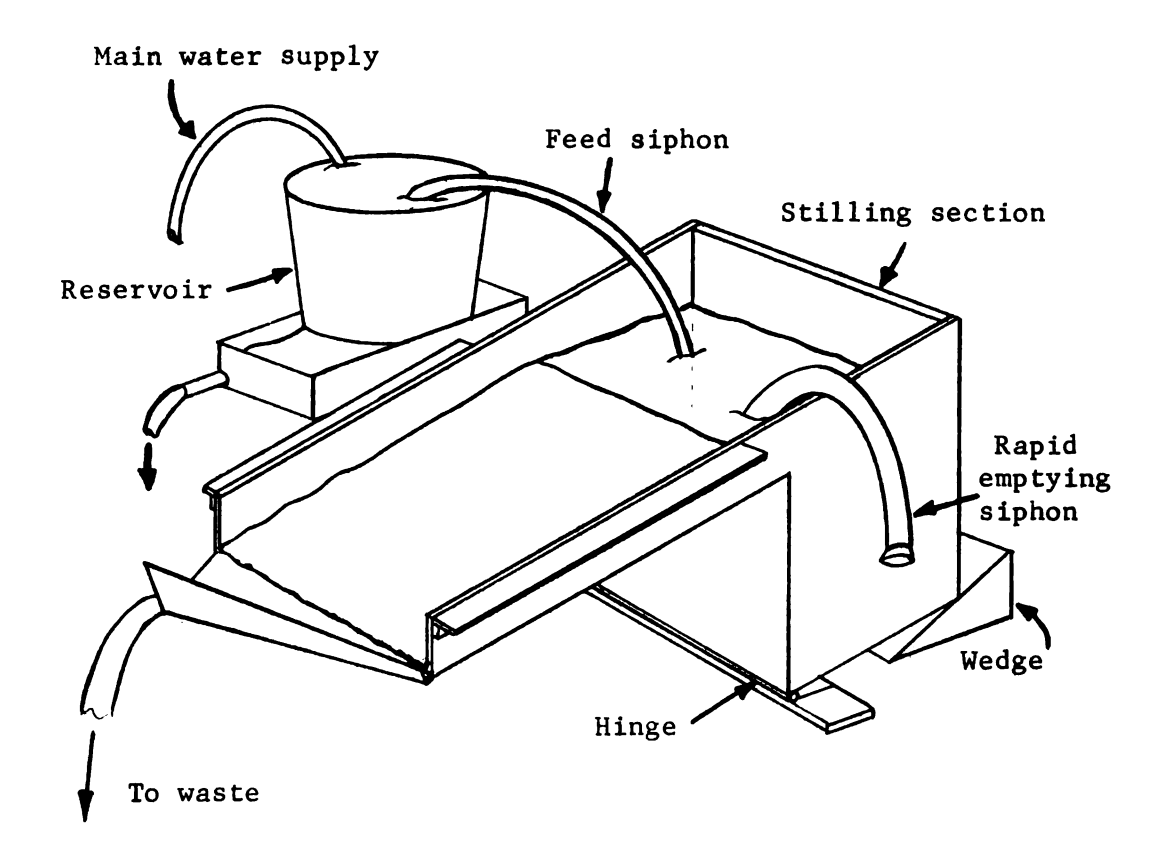


Figure 6. Diagram of apparatus used to produce thin film flow.

the surface by means of a micrometer gauge and pointer.

This gives accurate results in the absence of surface
waves, which was the case in the study.

The depth of the water was found by lowering the pointer to the channel bed until it resisted gentle turning. This ensured that the pointer was on the channel bed in all cases, especially when rough surfaces were used. A reading was then taken. The pointer was raised and lowered again until it just touched the surface of the water as determined by visual observation and another reading was taken. The flow depth was found by the difference in the two readings. The process was repeated several times to ensure a uniform film thickness existed in the channel. Preliminary testing showed a uniform flow across the channel and a profile similar to that shown in Figure 7 for all cases tested.

Construction of the Bed Plates

From preliminary calculations, it was considered that even the finest particles (having a diameter of 4.0 microns) should settle out in 11.5 cm (see Appendix B). Preliminary testing indicated that the actual distance of transport was of the order of about 10 cm. A bed length of 60 cm. was chosen to provide a length of slope having uniform flow conditions in which experimentation could be performed. The bed plates were made 30 cm. wide to fit the flow channel.

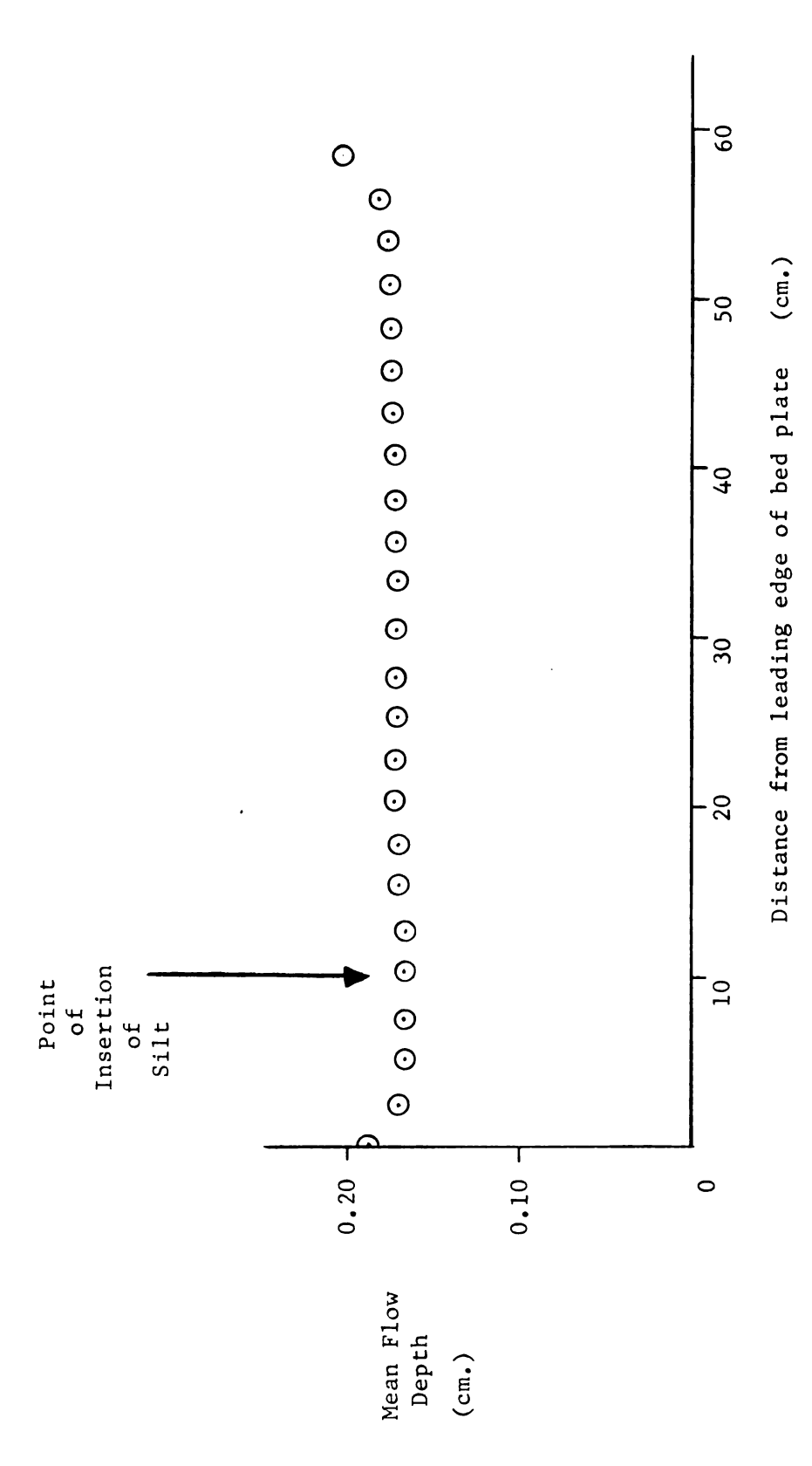


Figure 7. Graph of typical flow profile down bed plate. Note position of insertion of silt 10 cm. from leading edge of bed plate.

gauge steel was cut to size to provide a stiff backing.

Strips of abrasive belting were glued to the steel plate using waterproof glue. Care was taken to produce a smooth surface and to ensure that the edges of the strips were firmly attached to prevent the entry of water. The surfaces were pressed together and left to dry for several hours.

After drying the surface was checked to ensure smoothness and uniformity. Surfaces with local variations of more than 0.1 cm. were discarded. The center-line of the flow path was marked in pencil and it was divided into 2.5 cm. segments. It was determined during preliminary tests that this division of the deposited traces gave adequate samples for the analysis.

After trimming, the surface was coated with six coats of Krylon clear lacquer spray, which provided adequate waterproofing. However, it was found that in order to minimise the effects of the surface tension of water, it was necessary to roughen the surface with fine sand. Water was applied during this process, and the sand was gently rubbed across the lacquered surface by hand. This caused a very slight roughening of the lacquered surface and allowed the water film to spread uniformly.

It was found that bed plates produced in this way performed satisfactorily and could withstand periods of immersion in water of up to 30 minutes without apparent

signs of deterioration. These surfaces also allowed easy removal of deposited silt after drying. Two rough surfaces were made as indicated and used in the investigation. The abrasive belting used was a product of Minnesota Mining and Manufacturing Company. To produce a medium sand surface an 80-grade belting was used. For a very coarse sand surface a 40-grade belt was found satisfactory.

Instrumentation

The depth measuring device consisted of a micrometer gauge and a pointer, as described earlier. The micrometer gauge has an accuracy of ±0.0025 cm. The flow velocity was measured by placing a 1000 ml. measuring cylinder under the drain outlet of the bed section. The time for 1000 ml. was measured with a hand-held stopwatch, with an accuracy of ±0.1 sec. The flow velocity was measured at least four times to ensure uniformity, and the results averaged.

To analyse the sediment samples a Coulter Counter
Industrial Model B was used. The Coulter Counter determines
the number and size of particles suspended in an electrically
conductive liquid. This is done by forcing the suspension
to flow through a small aperture having an immersed electrode on either side. As a particle passes through the
aperture, it changes the resistance between the electrodes.
This produces a short duration voltage pulse having a
magnitude proportional to the particle volume. During

analysis of a sample the series of pulses is electronically scaled and counted.

The pulse height and instrument response are essentially proportional to the particle volume, and to fluid resistivity for particles up to 30 to 40 per cent of the aperture diameter. The particle resistivity has negligible effect. The principal does not permit significant discernment of particle shape, and results are expressed in equivalent spherical diameters. This proves acceptable as sufficiently high numbers of particles traversing the aperture. The theory of operation of the Coulter Counter is simple and side effects are negligible. The instrument is simple to calibrate. Calibration and sample analysis procedures are given in Appendix A.





Figure 8. The Coulter Counter Industrial Model B.

Above: (a) General view of Coulter Counter. Below: (b) Close-up of aperture tube stand.

TEST PROCEDURES

Flow Test Procedures

Tests were conducted in a research laboratory with a mean temperature of approximately 20°C. Attempts were made to protect the bed surface from foreign matter at all times. This was to protect the Coulter Counter aperture from blockage. All tests were conducted in the following manner:

- 1. The water was turned on and run for approximately 15 minutes to ensure a constant water temperature. The mean water temperature during testing was about 13° C.
- 2. The reservoir and stilling section were thoroughly cleaned to remove material that might cause blockage of the Coulter Counter aperture.
- 3. The rapid-emptying device was also cleaned and one end blocked with a rubber plug. It was filled with water and placed in the stilling section.
- 4. The bed plate was thoroughly cleaned, dried and put in place. The edges were sealed with a plastic sealing tape to prevent seepage round the plate, which would introduce an error into the flow rate and the measured flow depth.

- 5. The bed was checked for alignment and the value of the bed slope was set. The reservoir and stilling section were filled with water.
- 6. The siphon was chosen, cleaned, filled and put in place.
- 7. The bed slope was adjusted for uniform slope.
 A 10 cm. long level was used to detect local variations.
- 8. The water was allowed to run, and the temperature was taken periodically until a constant water temperature was reached. The temperature was noted.
- 9. The flow rate was obtained by measuring the time taken to fill a 1000 ml. measuring cylinder. The measurement was repeated four times, and the values noted.
- 10. The depth of flow was measured at a point 30 cm. from the upper edge of the bed plate, and in the line of flow to be used in the test. One location was chosen to take the flow depth measurement since this reduced the time taken for the experimental run. It was considered necessary to avoid a change in the flow rate due to the collection of air bubbles in the siphon, and also to avoid possible deterioration of the rough surfaces during prolonged immersion in water. From

Figure 7 it can be seen that this gives a measure of the flow depth over the area used in the experiment, with a maximum error of ±0.005 cm. This measurement was repeated twice and the results averaged.

- 11. The flow rate was measured two more times.
- 12. The temperature was checked to ensure no variation was occurring.
- 13. The silt suspension was thoroughly agitated to ensure complete suspension. An eye dropper was quickly filled with the suspension.
- 14. The first drop was released into a beaker containing 125 ml. of 2 per cent potassium chloride solution. It was quickly covered with transparent plastic to exclude impurities. The suspension thus prepared was used as a standard in the analysis of each run.
- 15. The eye dropper was held at the 10 cm. mark, about 0.5 cm. above the water surface and 10 drops of the suspension were rapidly released.

 An average time for this to take place was 6 seconds.
- 16. A delay of 5 seconds was allowed before the rapid-emptying siphon plug was removed. The water level in the stilling section dropped below the bed level almost immediately.

- 17. The siphons were removed and the water supply turned off.
- 18. The excess water was allowed to drain from the plate for a few minutes and the sealing strips around the bed plate were removed.
- 19. The bed plate was quickly removed and dried so that the deposited material could be removed for analysis.

Sample Analysis

- The bed plate was placed in a room with a minimum draft and dust environment, and was allowed to dry for about two hours.
- 2. After this time the plate was set up at a slight angle (approximately 10°) in two directions at right angles.
- 3. Using the squegee as shown in Figure 5, the sample was washed into a clean dry dust-free beaker with 2% potassium chloride solution.

 The squegee was positioned and pressure applied so that only the deposited material was washed away and collected.
- 4. The sample area from which the sediment was being removed was lightly agitated with a small short-haired brush. The brush was washed and put aside and the sample area rewashed with potassium chloride solution.

- 5. The volume of potassium chloride solution was made up to a total volume of 125 ml. and the beaker quickly covered with a transparent plastic sheet to prevent the entry of impurities into the sample.
- 6. The process was repeated for 2.5 cm. strips of the silt trace down the bed trace until the trace became indistinct.
- 7. The samples were then analyzed with the Coulter Counter as given in Appendix A.

Table 4. Sample Of Coulter Counter Data

Run No. 14

Slope 3% Surface: 80 - Grade

Dis	tanc	e Dow	n Slop	e: 7.62	cm		MEAN RAW	VOLUME V_= ht_IA (CUBIC	EQUIVALENT SPHERICAL DIAMETER
$^{\mathrm{T}}_{\mathrm{L}}$	I	Α		RAW COU	NTS		COUNT	MICRONS)	d _L (MICRONS)
(A)	(B)	(C)	*1 (D)	* ₂ (E)	*3 (F)	* ₄ (G)	× (H)	(1)	(J)
20	4	64	26	23	17	18	21.0	30617.6	38.215
20	2	64	194	166	167	199	181.5	15308.8	31.064
20	1	64	629	591	657	615	623.0	7654.4	24.660
20	1	32	1396	1322	1261	1326	1326.25	3827.2	19.577
20	1	16	2178	2131	2157	2088	2138.5	1913.6	15.532
20	1	8	2911	2971	2864	2870	2904.0	956.8	12.372
20	1	4	3390	3422	3341	3432	3396.25	478.4	9.788
20	1	2	3771	3916	3827	3766	3820.0	239.2	7.764
20	1	1	4222	4334	4140	4227	4230.75	119.6	6.166
20	1	1/2	5262	5464	5265	5398	5347.25	59.8	4.755

Table 5. Analysis of Data From Table 4

EQUIVALEN SPHERICAL DIAMETER (MICRONS) d L	MEAN RAW	COUNT DIFFERENCE *2 - *1	MEAN EQUIVALENT SPHERICAL DIAMETER d (MICRONS)
20 215	21 0		
38.215	21.0	160.5	34.64
31.064	181.5	441.5	27.49
24.660	623.0		
19.577	1326.25	703.25	21.83
15.532	2138.5	812.25	17.32
		765.5	13.74
12.327	2904.0	492.25	10.91
9.788	3396.25		
7.764	3820.0	423.75	8.66
6.166	4230.75	410.75	6.87
		1116.5	5.46
4.755	5347.25		

DATA ANALYSIS

Most of the measurements taken to establish experimental conditions were repeated several times and averaged as indicated in the test procedures. The principal data reduction was concerned with the results from the Coulter Counter.

The calculation of the calibration constant is given in Appendix A. The value used in this study was h = 5.89 and was found to vary only slightly during the series of experiments giving a variation in mean particle diameter values of ± 1 micron.

A sample of the data obtained from the Coulter Counter is given in Table 4. The significance of each column is given by reference to the identifying letter.

- (A) The threshold setting t_L
- (B) The aperture current setting I
- (C) The amplification setting A
- (D), (E), (F), (G) The four counts obtained at the above settings (x_1, x_2, x_3, x_4)
- (H) The mean count $\bar{x} = \frac{1}{4}(x_1 + x_2 + x_3 + x_4)$
- (I) The volume of the smallest particle registering on the counter at the settings given

$$v_{T_i} = ht_{T_i} IA$$

(J) The equivalent spherical diameter of the particle whose volume is given in condition (I)

$$d_{L} = 1.241 \sqrt[3]{v_{L}}$$

The sample of data analysis given in Table 5 is continued from Table 4.

To find the number of particles in the sample in a given size range, the difference between two adjacent values of the mean count \overline{x} was determined for example, from Table 5:

 $x_1 - x_2 = \overline{x}$ = the number of particles in the size range $d_2 - d_1 = \overline{d}$ microns.

The operation of averaging the limits of the particle size implied that there were \overline{x} particles of dize \overline{d} in the sample.

To find the particle size distribution, the values of \overline{x} were divided by the total number of particles in the sample. A percentage size distribution for each sample was obtained. However, it is necessary to relate all the samples. This was achieved by comparing all the samples of the run to the master silt analysis, which was obtained from the analysis of the sample of suspended material taken before each run. The master silt sample was analyzed in the manner given in Appendix A and the results processed as given above. The number of particles in each size range of the master silt sample was multiplied by 10 since 10 drops of suspended material were used in each test. The

result gave the total number of particles present initially in the test. By dividing the particles of a particular size in a given sample by the total number of particles of that size, a percentage of the total particles deposited at a location was obtained.

In this manner the deposition curves for particles of given size can be obtained for each run, which is given in numerical form in Appendix C, and an example of which is given graphically in Figure 9. The distance from the point of insertion of the suspended material to its point of maximum deposition is called the Critical Distance X. Its value can be extracted from the data and is given in each case in Appendix C. The values obtained for the Critical Distance X are compared against the theoretical models described earlier.

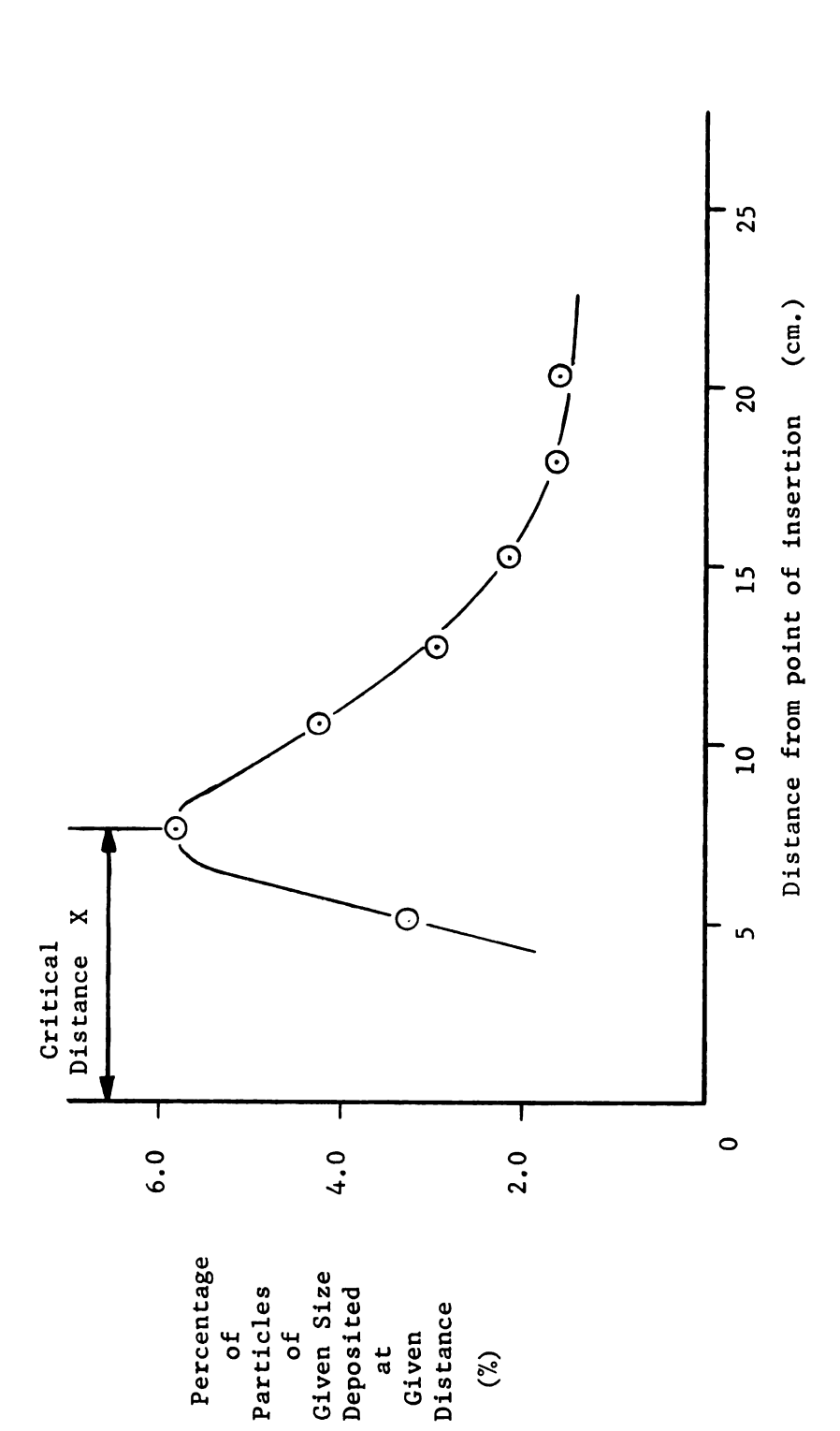


Figure 9. Typical deposition curve for a particular particle size. Distance from point of application to point of maximum deposition for the particle size is referred to as Critical Distance. (Deposition of 17.3 micron particles on glass bed plate at 3% slope with medium flow.)

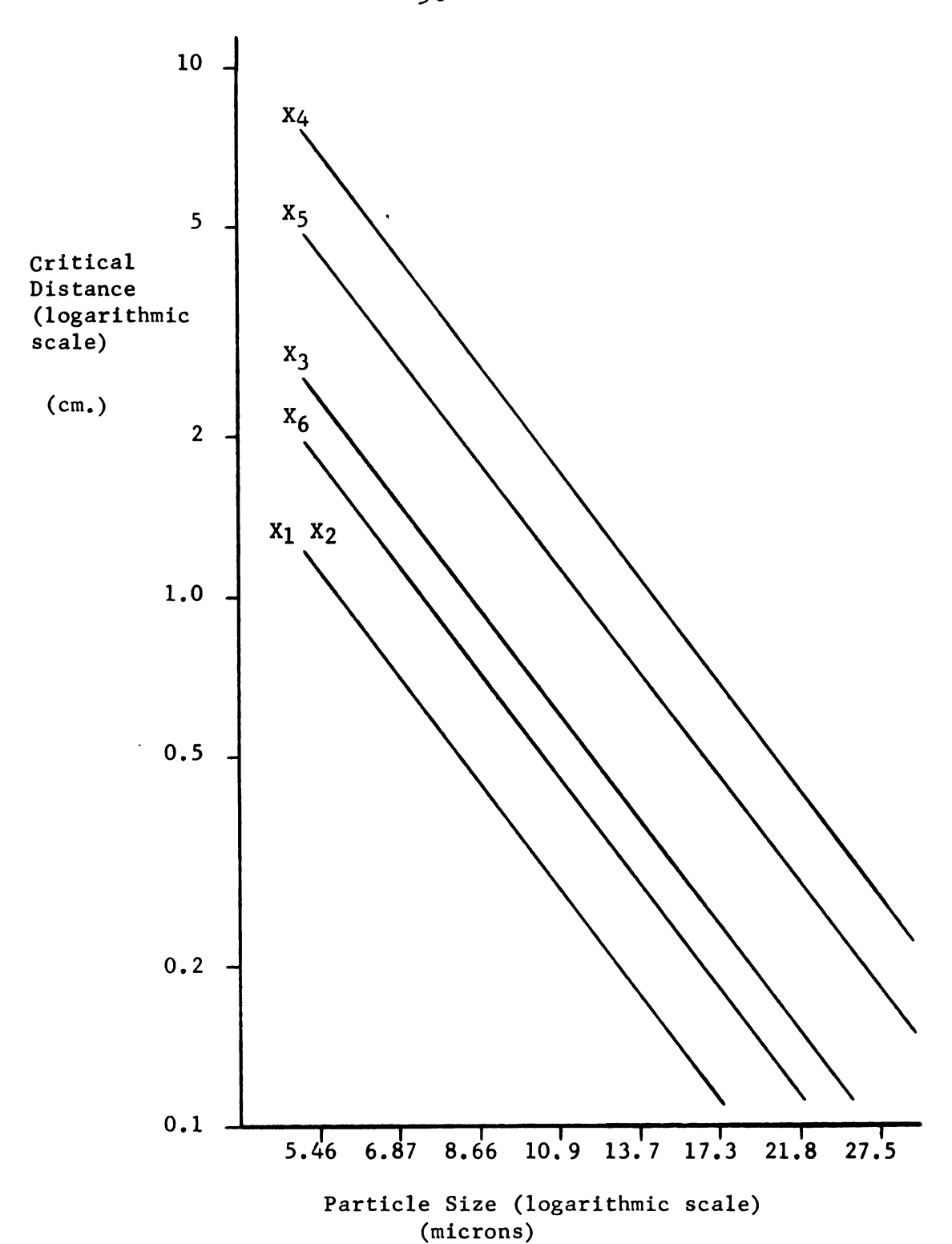


Figure 10. Graphs of theoretical models having the general form:

$$X = \frac{K}{k c^2}$$

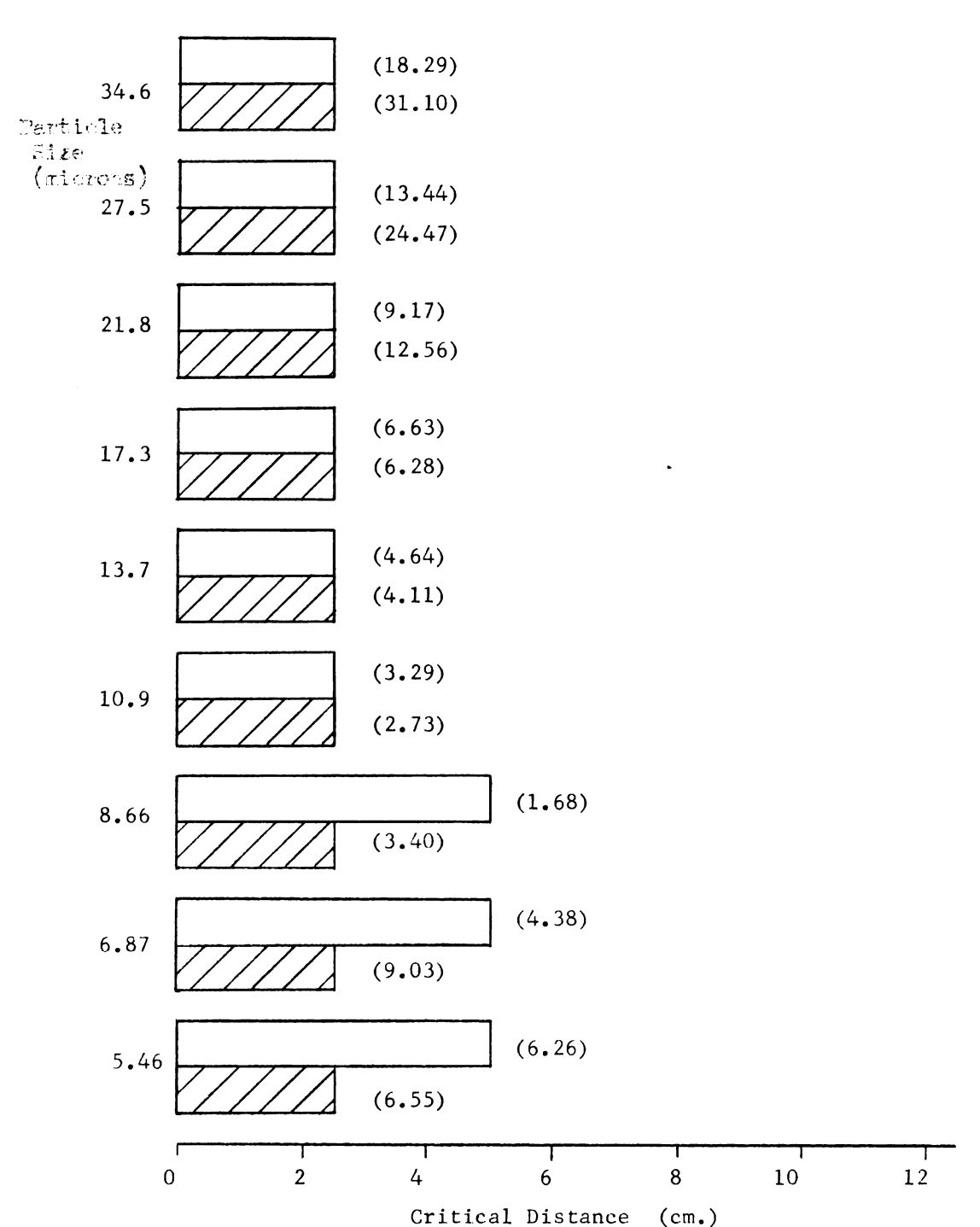
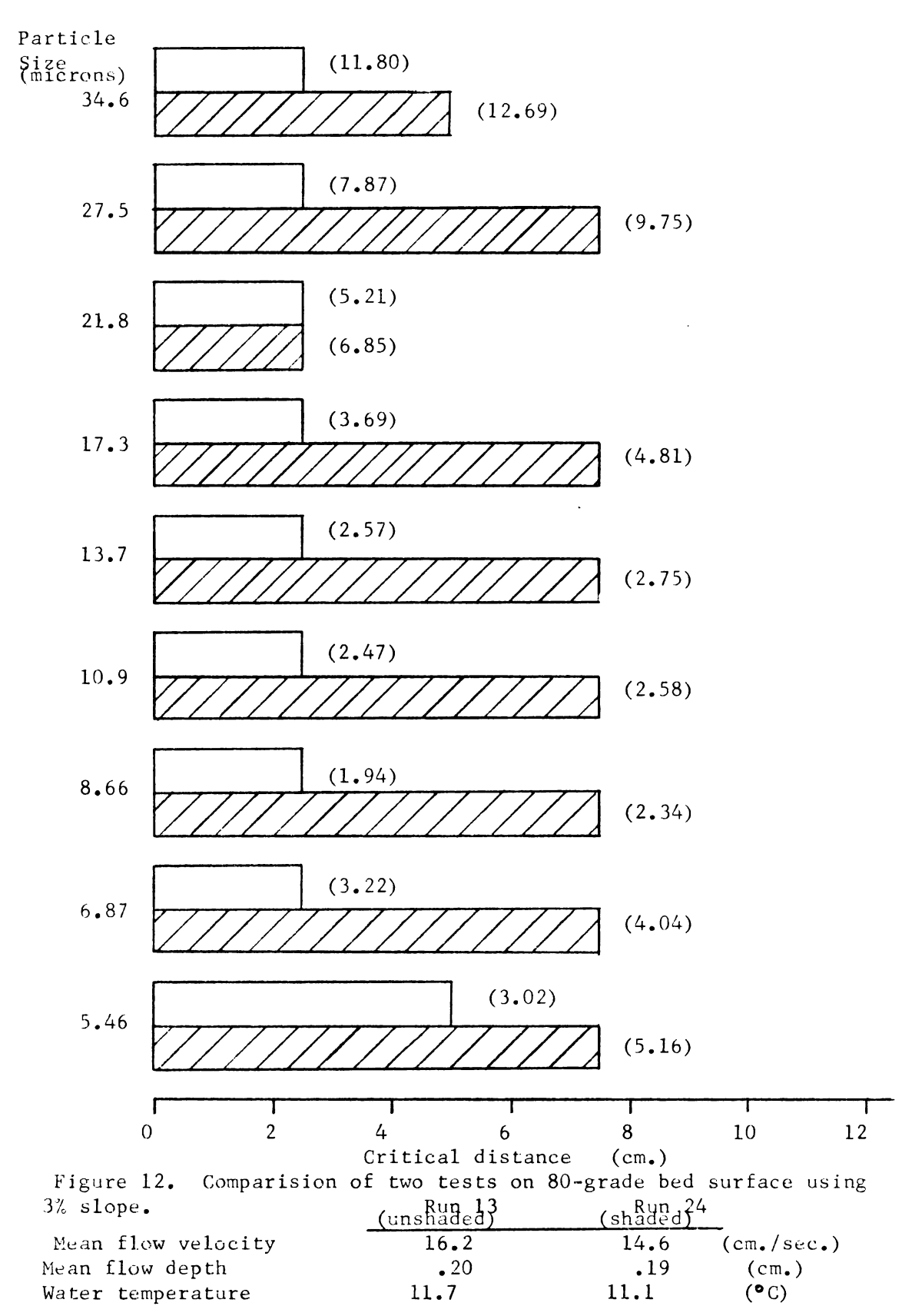
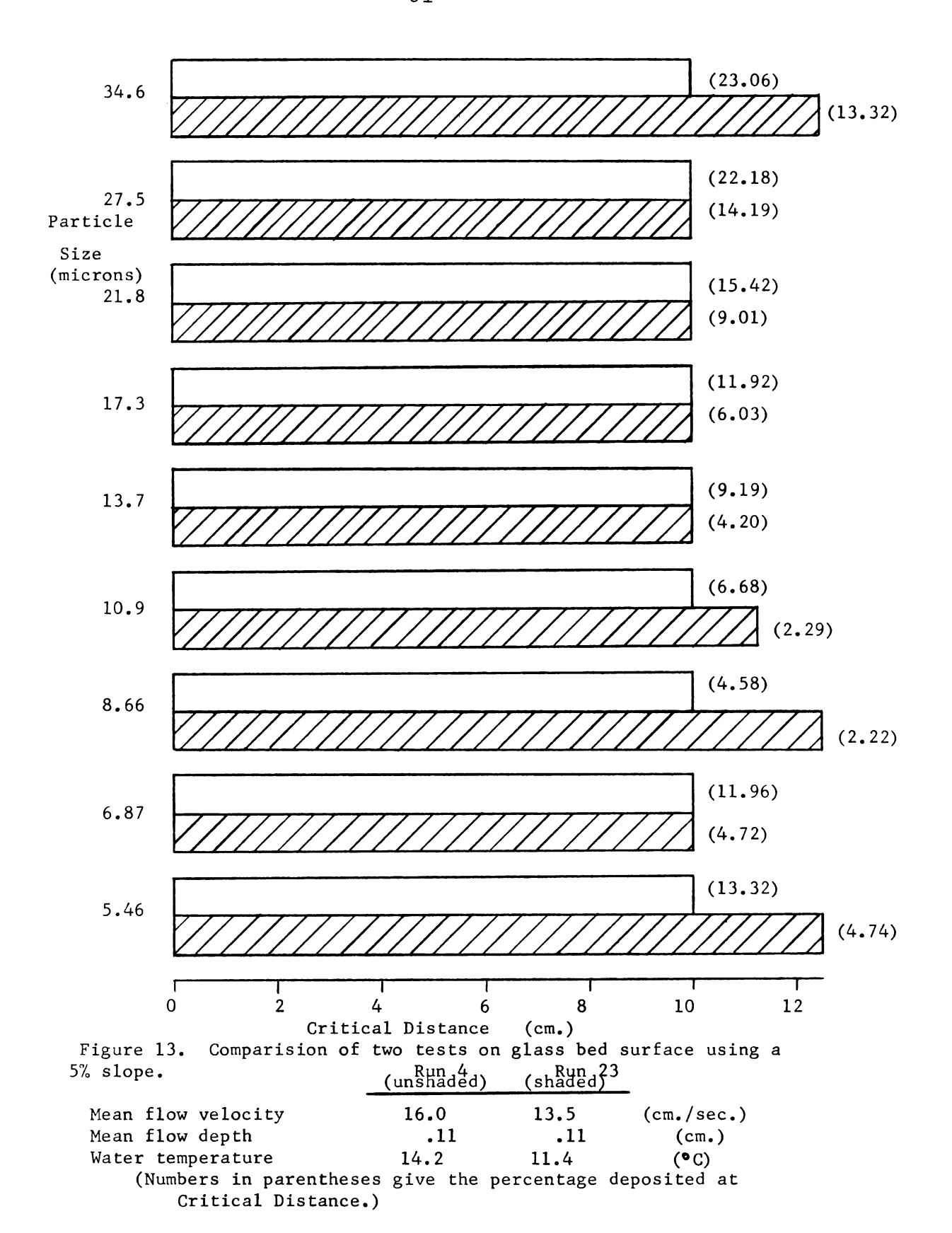


Figure 11. Comparision of two tests on 40-grade using 1% slope.

	(unshaded)	(shaded)	
Mean flow velocity	8.7	8.5	(cm./sec.)
Mean flow depth	. 27	. 28	(cm.)
Water temperature	11.1	11.4	(°C)





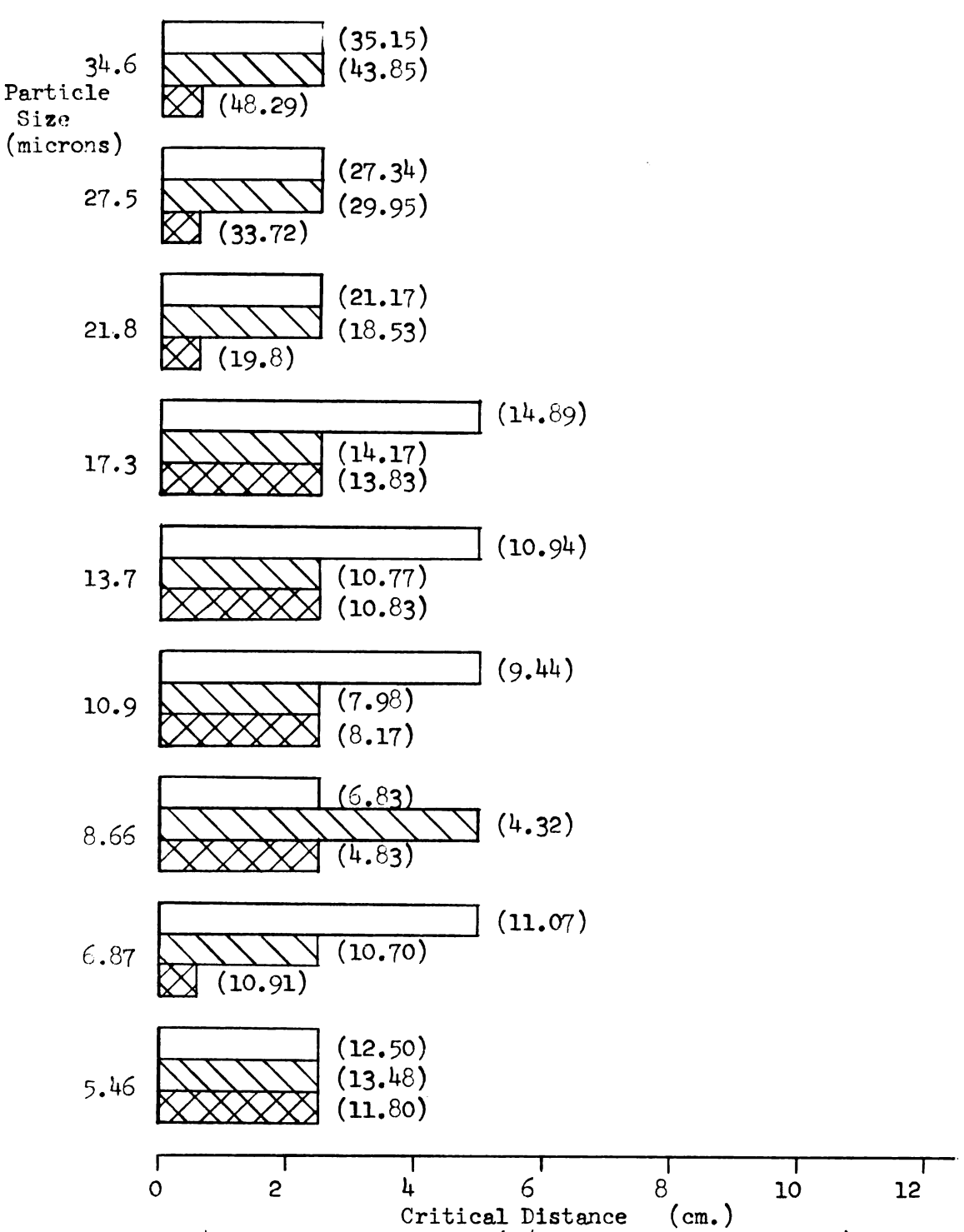


Figure 14. Comparison of runs (1% bed slope and low flow)
Top to bottom: Run 8 - Glass, Run 12 - 80-grade, Run 22 - 40grade. See reduced data.

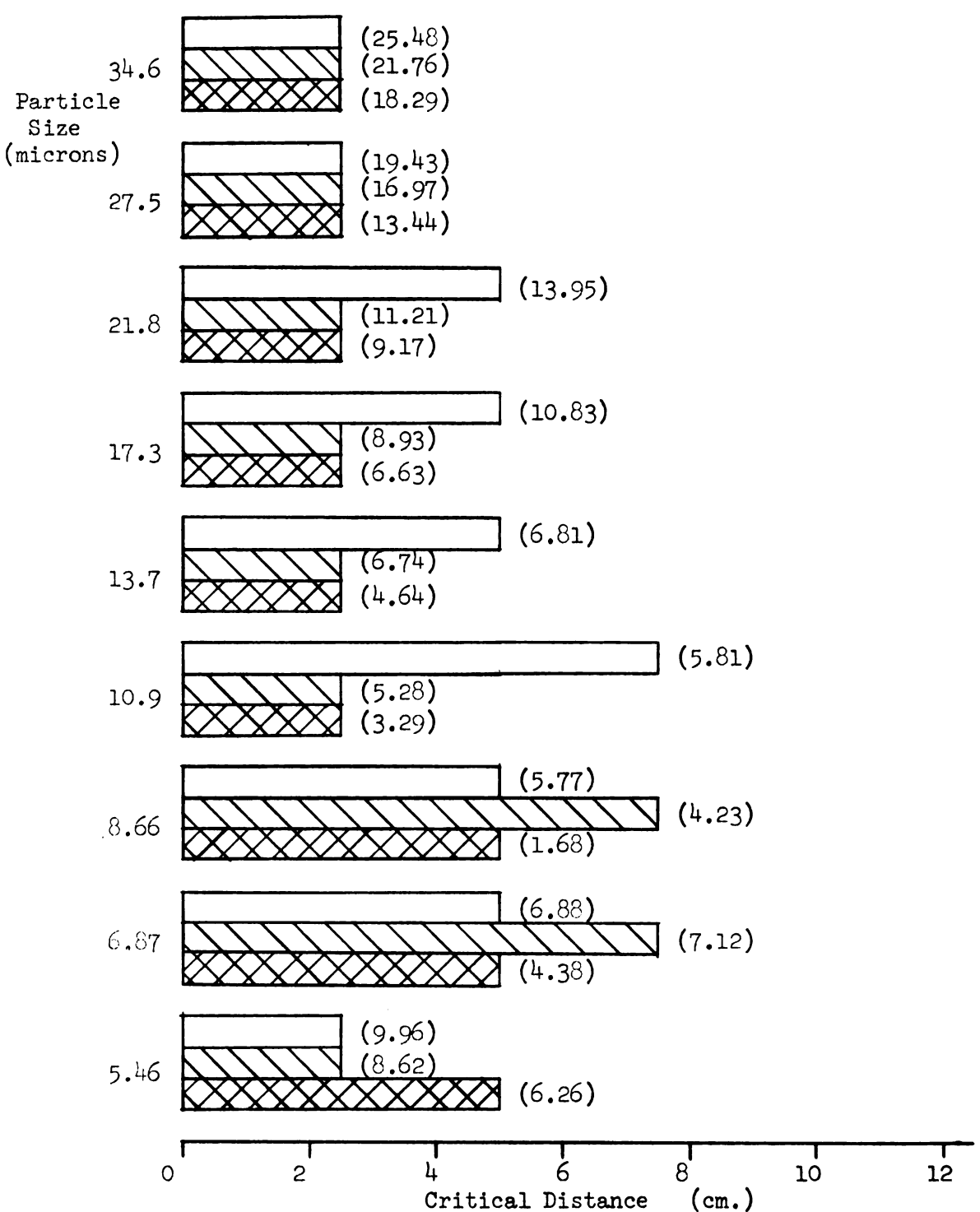


Figure 15. Comparison of runs (1% slope and medium flow)
Top to bottom: Run 6 - Glass, Run 10 - 80-grade, Run 21 - 40grade. See reduced data.

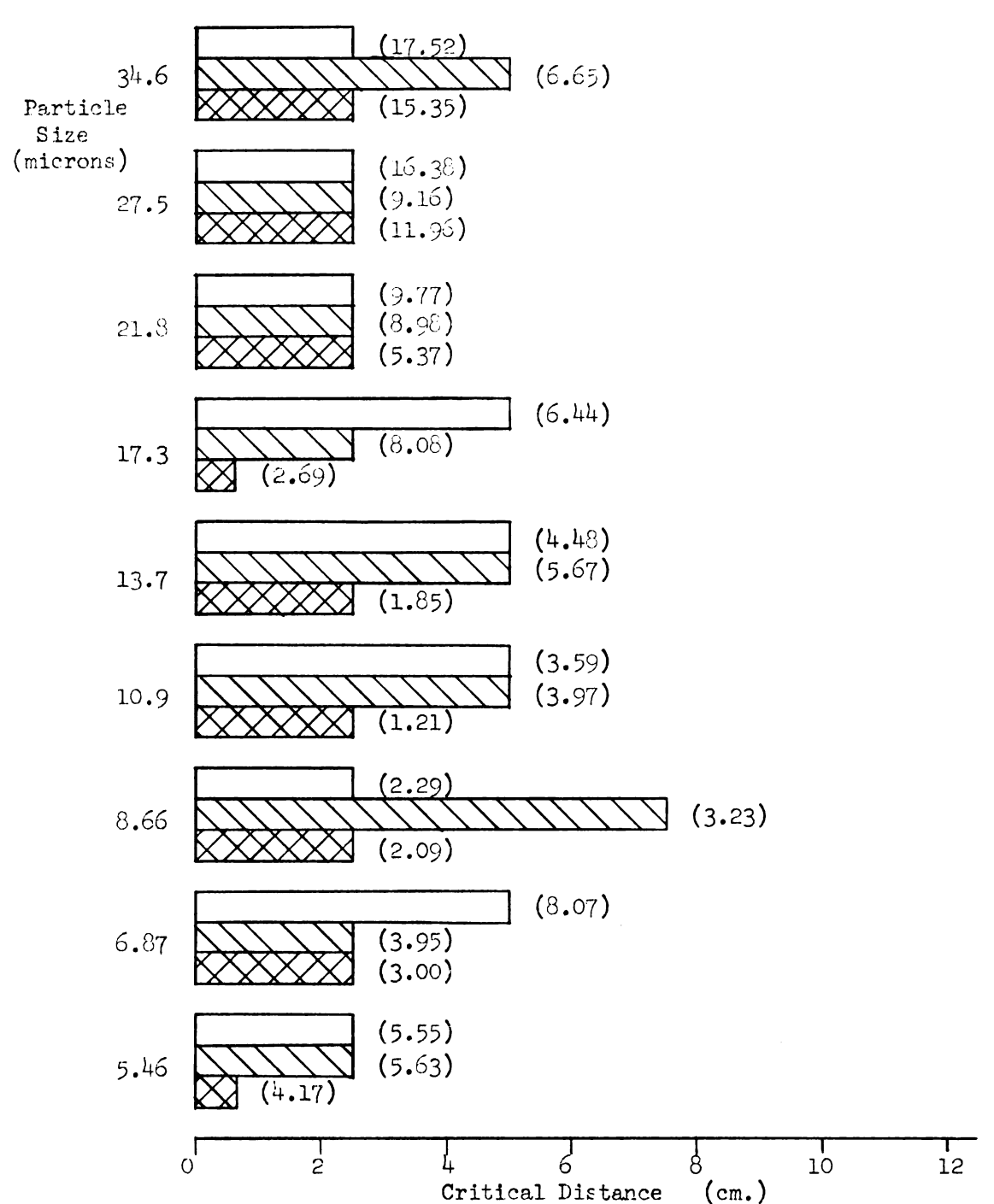


Figure 16. Comparison of runs (3% slope and low flow)
Top to bottom: Run 16 - Glass, Run 14 - 80-grade, Run 20 - 40grade. See reduced data.

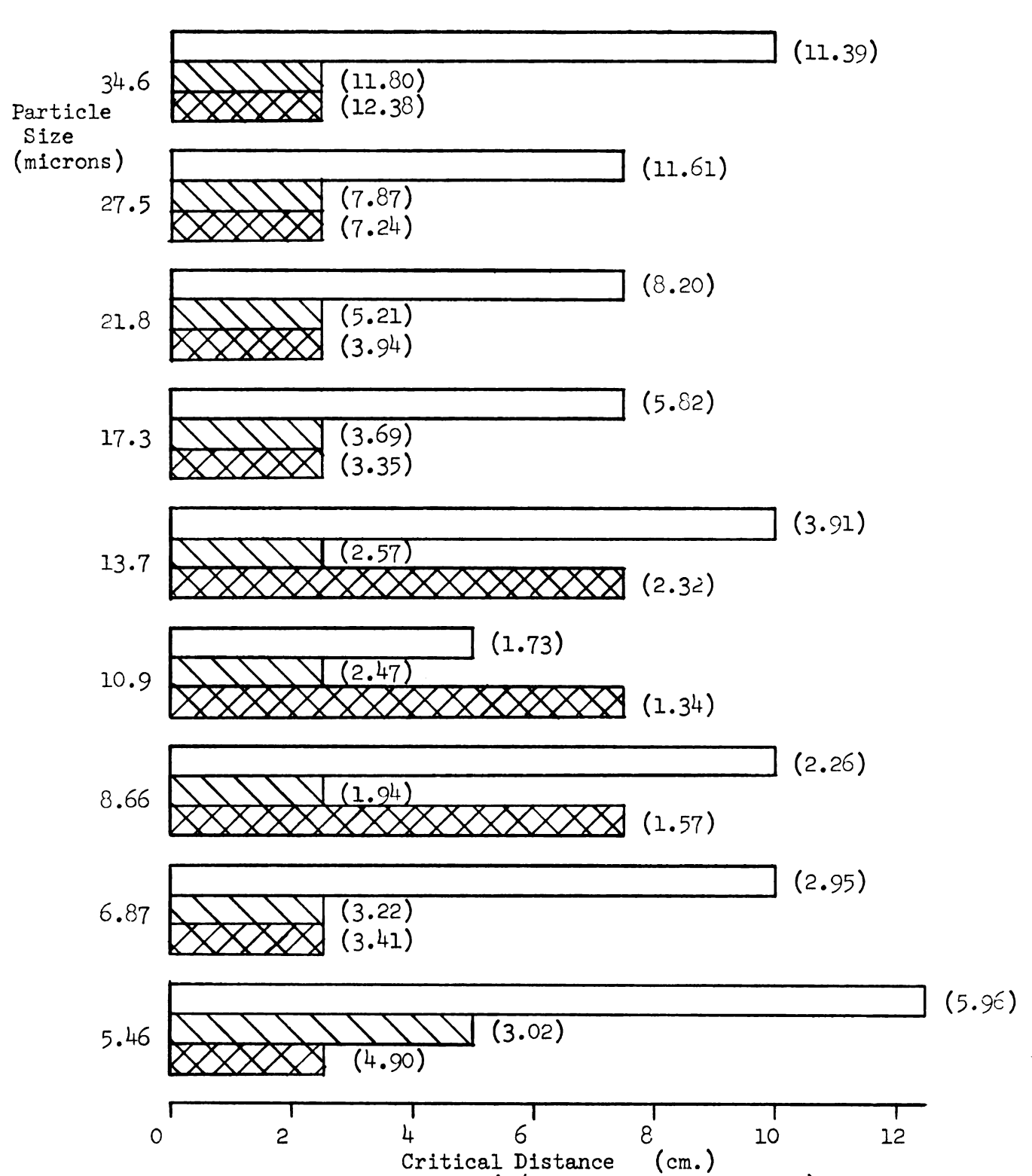


Figure 17. Comparison of runs (3% slope and medium flow)
Top to bottom: Run 15 - Glass, Run 13 - 80-grade, Run 19 - 40grade. See reduced data.

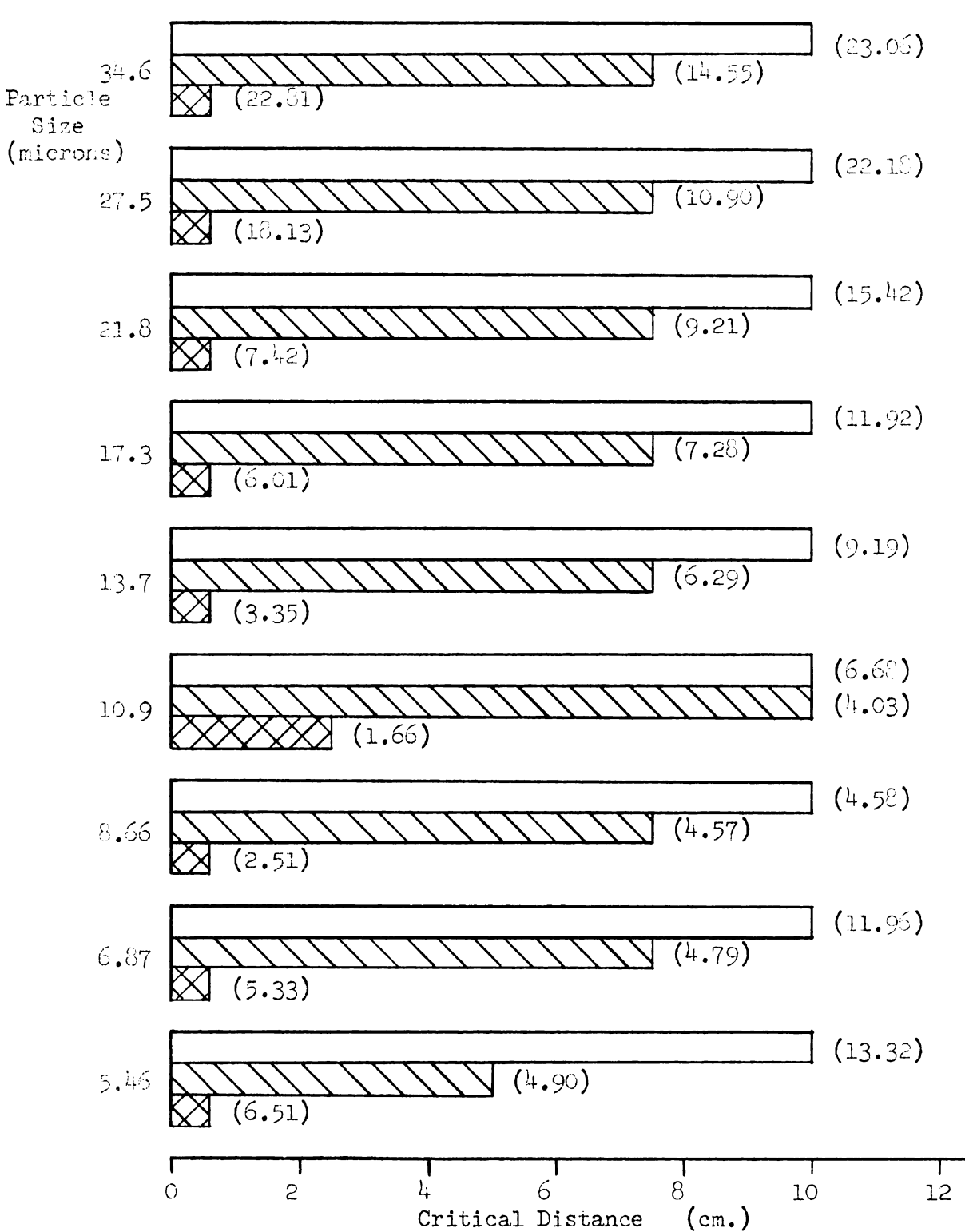


Figure 18. Comparison of runs (5% slope and low flow)
Top to bottom: Run 4 - Glass, Run 11 - 80-grade, Run 18 - 40grade. See reduced data.

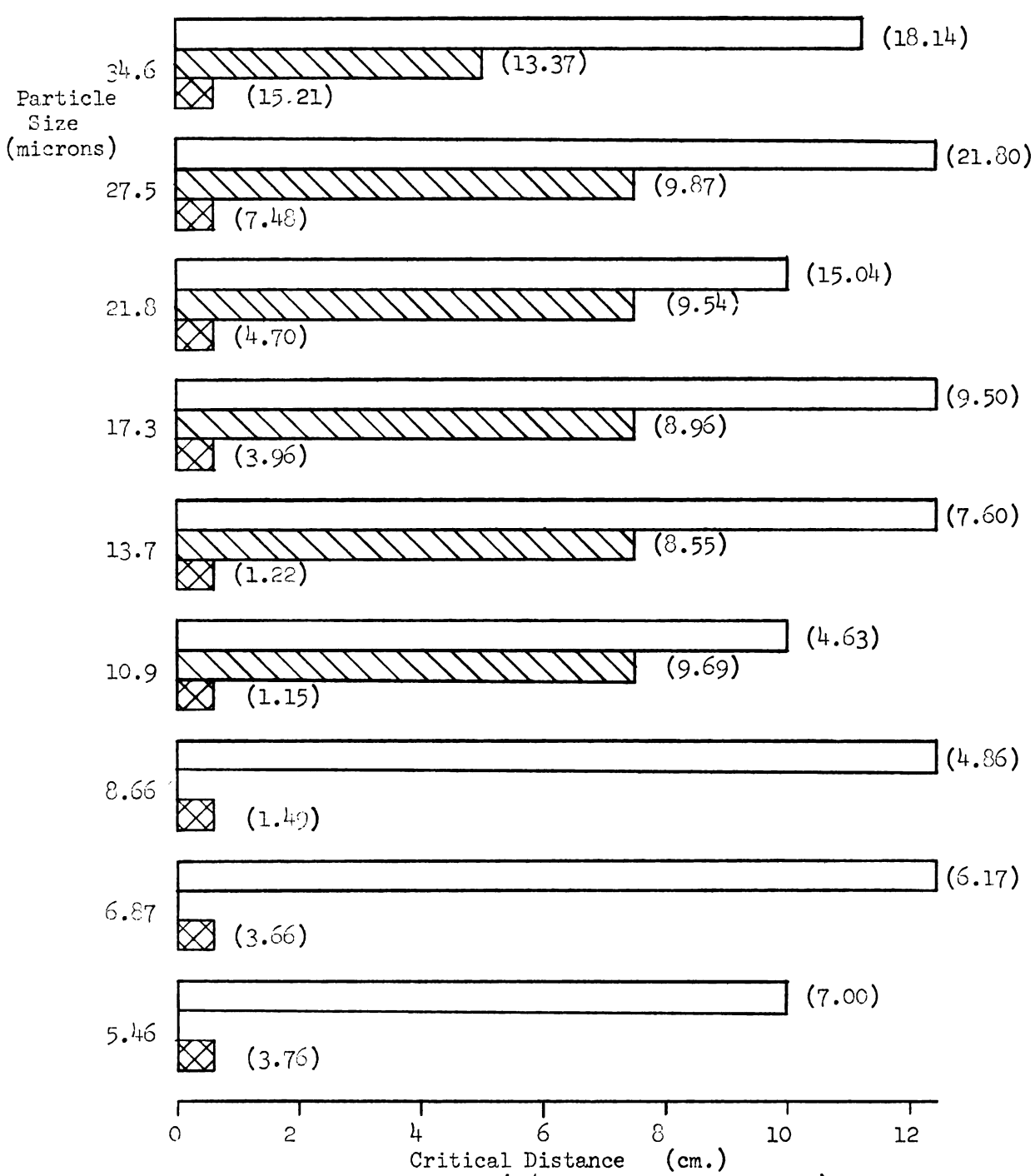


Figure 19. Comparison of runs (5% slope and medium flow)
Top to bottom: Run 3 - Glass, Run 9 - 80-grade, Run 17 - 40grade. See reduced data.

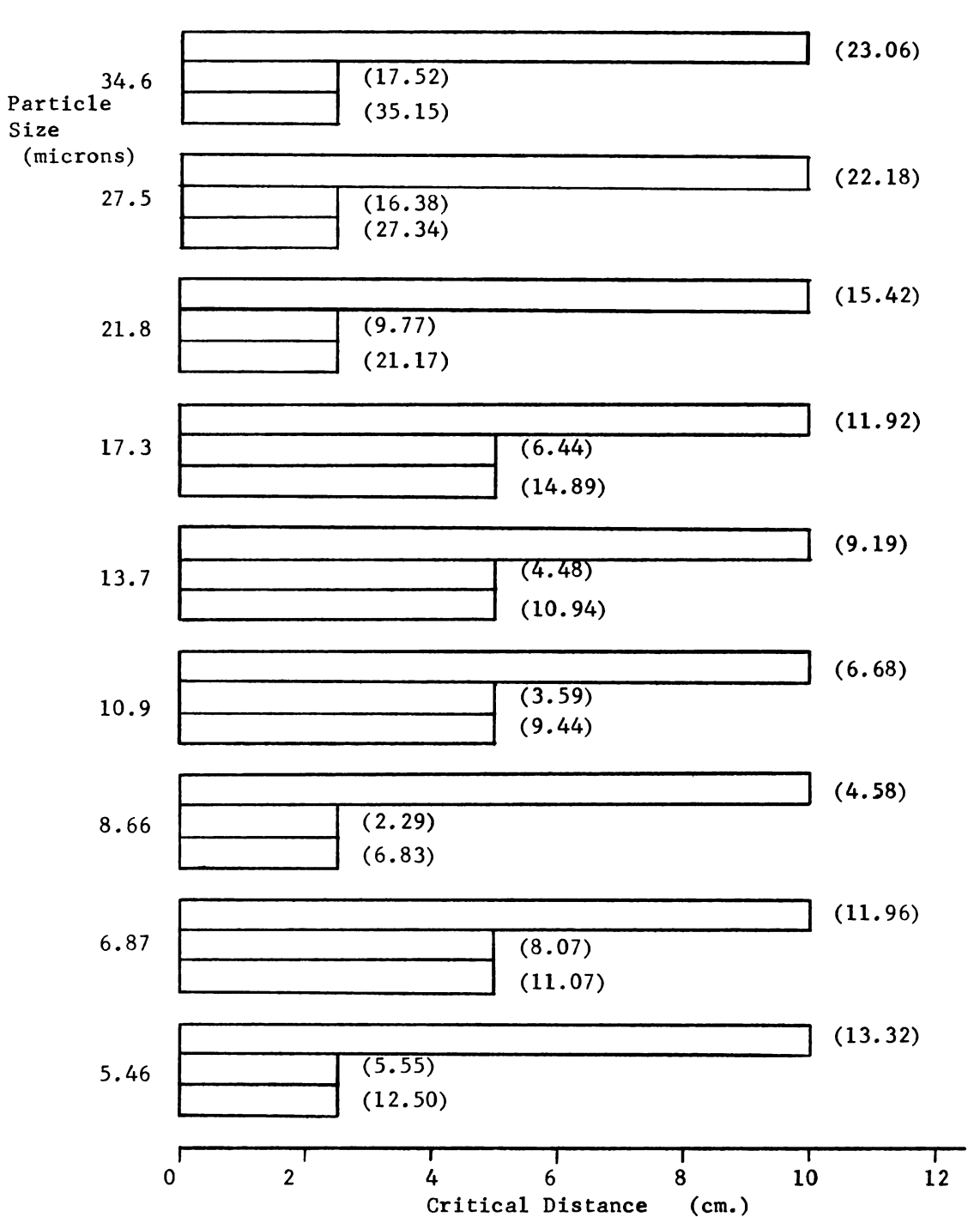


Figure 20. Comparison of slopes (glass bed and low flow) Top to bottom: Run 4 - 5%, Run 16 - 3%, Run 8 - 1%. See reduced data.

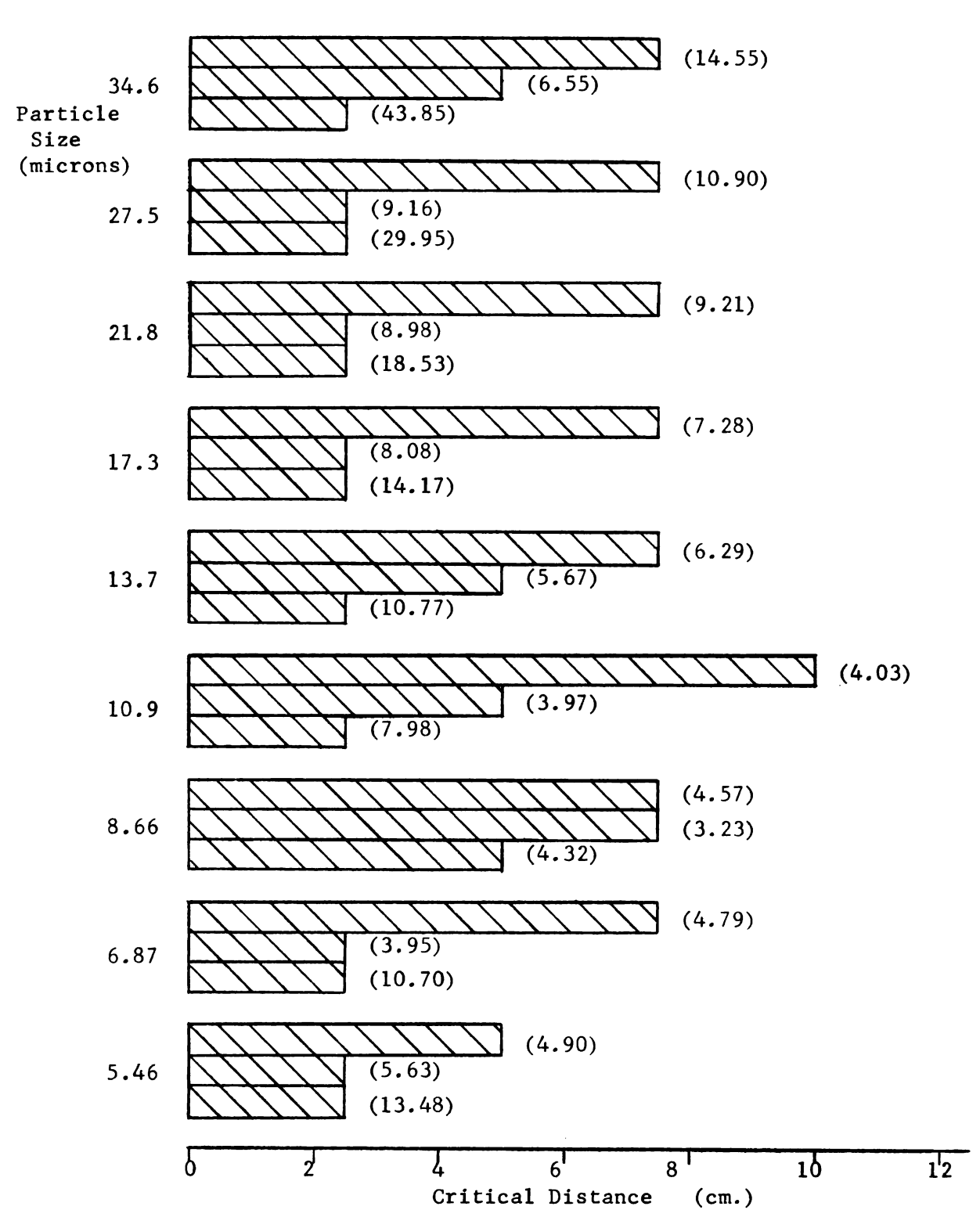


Figure 21. Comparison of slopes (80-grade bed and low flow) Top to bottom: Run 11 - 5%, Run 14 - 3%, Run 12 - 1%. See reduced data.

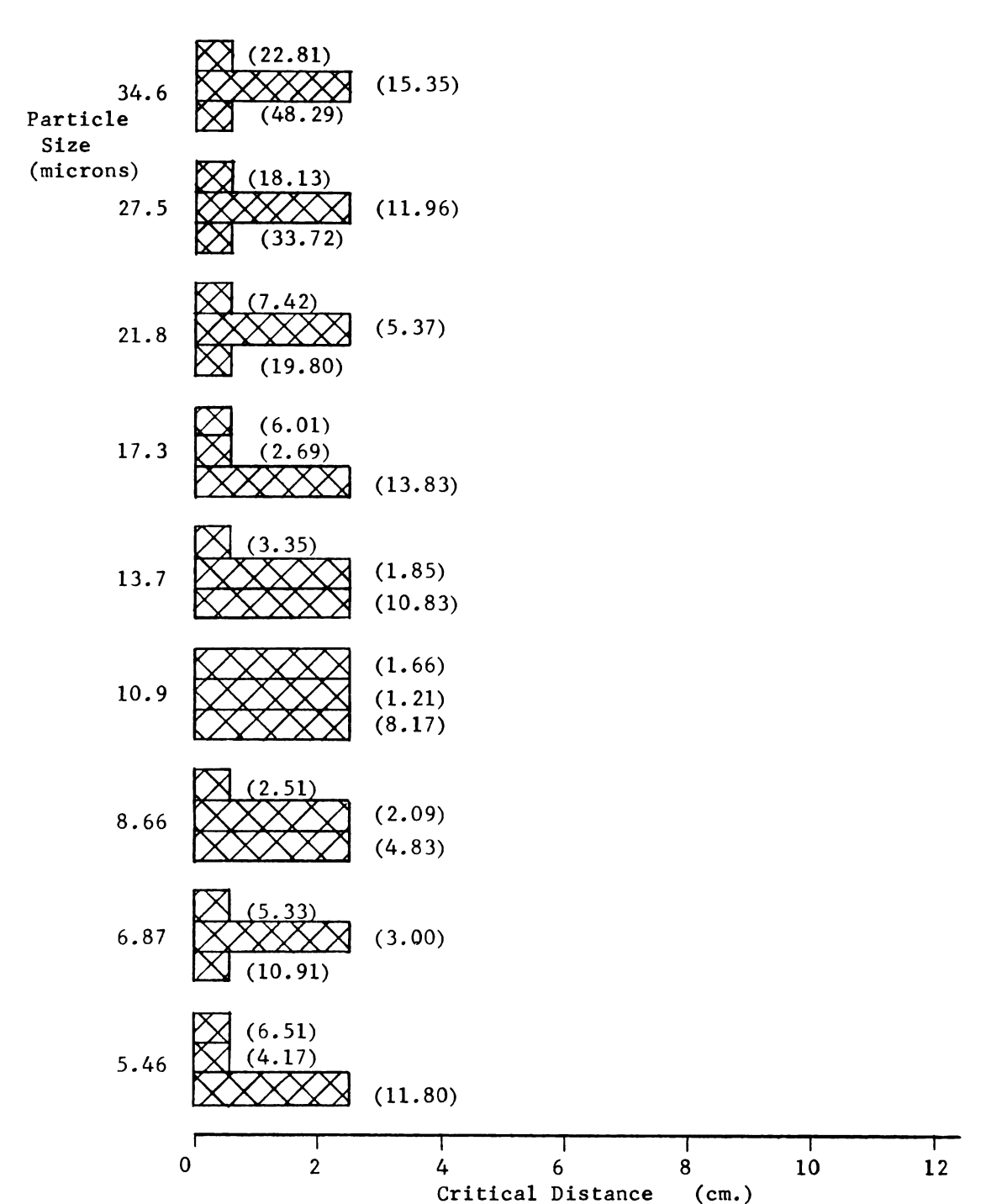


Figure 22. Comparison of slopes (40-grade bed and low flow) Top to bottom: Run 18 - 5%, Run 20 - 3%, Run 22 - 1%. See reduced data.

DISCUSSION OF RESULTS

A sample of the data obtained from the Coulter Counter is given in Appendix C followed by the reduced data from the 21 runs conducted. One run was performed for each of the eighteen conditions considered. Preliminary testing showed that results obtained corresponded closely, although variations in the composition of the silt suspension used made comparison difficult. Variations in the experimental conditions were also noted. As a check on the repeatability of the tests, three repeated runs were performed covering the range of the conditions tested. These are compared in Figures 11, 12, and 13. The numbers in parentheses give the percentage of the given particle size deposited at the Critical Distance.

The eighteen conditions under which the tests were conducted are as follows:

- 1. Three bed slopes (5%, 3%, 1%)
- 2. Three bed surfaces (glass, 80-grade, 40-grade)
- 3. Two flow conditions (low flow: siphon of 0.95 cm. I.D.; and medium flow: siphon of 1.27 cm. I.D.)

 The runs that were repeated were: (1) 40-grade, 1% slope,

5% slope, low flow.

medium flow; (2) 80-grade, 3% slope, medium flow; (3) Glass,

The runs shown in Figures 11 and 13 show good agreement. The runs for the two test on the 80-grade bed surface at 3% slope show greater variation probably due to the differences in experimental conditions.

The results are given in numerical form in Appendix C and in graphical form in Figures 14 to 22.

The theoretical models are given graphically in Figure 10. It was stated earlier that all the models have the general form

$$X = \frac{K}{kr^2}$$

The magnitude of K is determined from the particular model characteristics as given in the theoretical development. The values used to determine the values of K and k were taken from the mean values of the experimental data. The values were:

Mean depth \overline{D} = 0.188 cm. Standard deviation = 0.048 cm.

Mean velocity \overline{u} = 12.52 cm./sec. Standard deviation = 3.25 cm./sec.

Mean slope P = 0.03

Mean viscosity $\overline{\mu} = 1.26 \times 10^{-5} \text{ gm./cm. sec.}$

Mean kinematic viscosity $\overline{v} = 1.3 \times 10^{-2} \text{ cm}^2/\text{sec}$.

These give the following values when used in the models considered:

$$X_{1} = X_{2} = \frac{33.04}{r^{2}}$$

$$X_{3} = \frac{70.32}{r^{2}}$$

$$X_{4} = \frac{201.1}{r^{2}}$$

$$X_{5} = \frac{134.6}{r^{2}}$$

$$X_{6} = \frac{53.56}{r^{2}}$$

It is these equations which were graphed in Figure 10. When these models are compared to the experimental results for the Critical Distance X, as shown in Figures 14 to 19, it can be seen that the experimental values for X are not functions of particle diameter. The accuracy of measurement of X was limited by the necessity of having a sufficient amount of the deposited material to provide an accurate analysis with particle counts much greater than the background level. The accuracy of measurement of X was therefore ±1.25 cm., or half the distance sampled at any one time. Within these limits, the values of X obtained experimentally are approximately uniform with particle size for given experimental conditions. However, for given slope and flow conditions, the value of the Critical

Distance X appeared generally to decrease with increasing surface roughness.

From the models considered it is suggested by the use of Stoke's law that the Critical Distance X is a second order function of particle size. Under no conditions tested was this found to be true, and it is therefore concluded that either (a) Stoke's law is not applicable for thin film flow, or (b) that some other mechanism is involved which completely masks the effect of particle diameter.

From Figures 14 to 22, it can be seen that bed slope has an effect on the Critical Distance X. By averaging the values of X over particle diameters in each case as given in the results (Appendix C), and relating these values to bed slope, the Critical Distance is shown to be a function of bed slope P and surface roughness. Figures 14 to 19 show that for given conditions, the value of the Critical Distance X decreases as the bed surface roughness increases except for the conditions of low slope there is no apparent surface roughness effect. For increasing slope and flow the effect of surface roughness becomes more pronounced. A further investigation of surface roughness might clarify the relationship. Figures 20 to 22 show the relationship of slope and surface roughness.

Although models (3) and (6) are functions of bed slope P, the inclusion of this variable does not improve

the adequacy of this model, since the slope term serves only to change the intercept of the line and not its gradient.

An investigation of the values obtained for X showed that the values of X for particle diameters in the range 8 to 10 microns were greater than those obtained for particles outside this size range. The values obtained for particles other than those in the diameter range 8 to 10 microns were approximately constant for each condition given. This suggests that particles of the size range 8 to 10 microns are transported further than particles having diameters greater or less than this range.

In addition, when summing the proportions of each particle size retained, it was found that the total particle retention is related to particle size as shown in Figures 23 to 25. Those curves exhibit minimum total retention for particles in the size range 8 to 10 microns diameter indicated earlier. The spread in the values of total retention percentage is probably due to the variation in test conditions.

In order to test this phenomenon against a possible theoretical model, the parameters for the third order relationship between velocity and depth were arranged so that the velocity profile gave the "zero net vertical force" value for particles in the size range 8 to 10 microns. The value was obtained using model (4). This

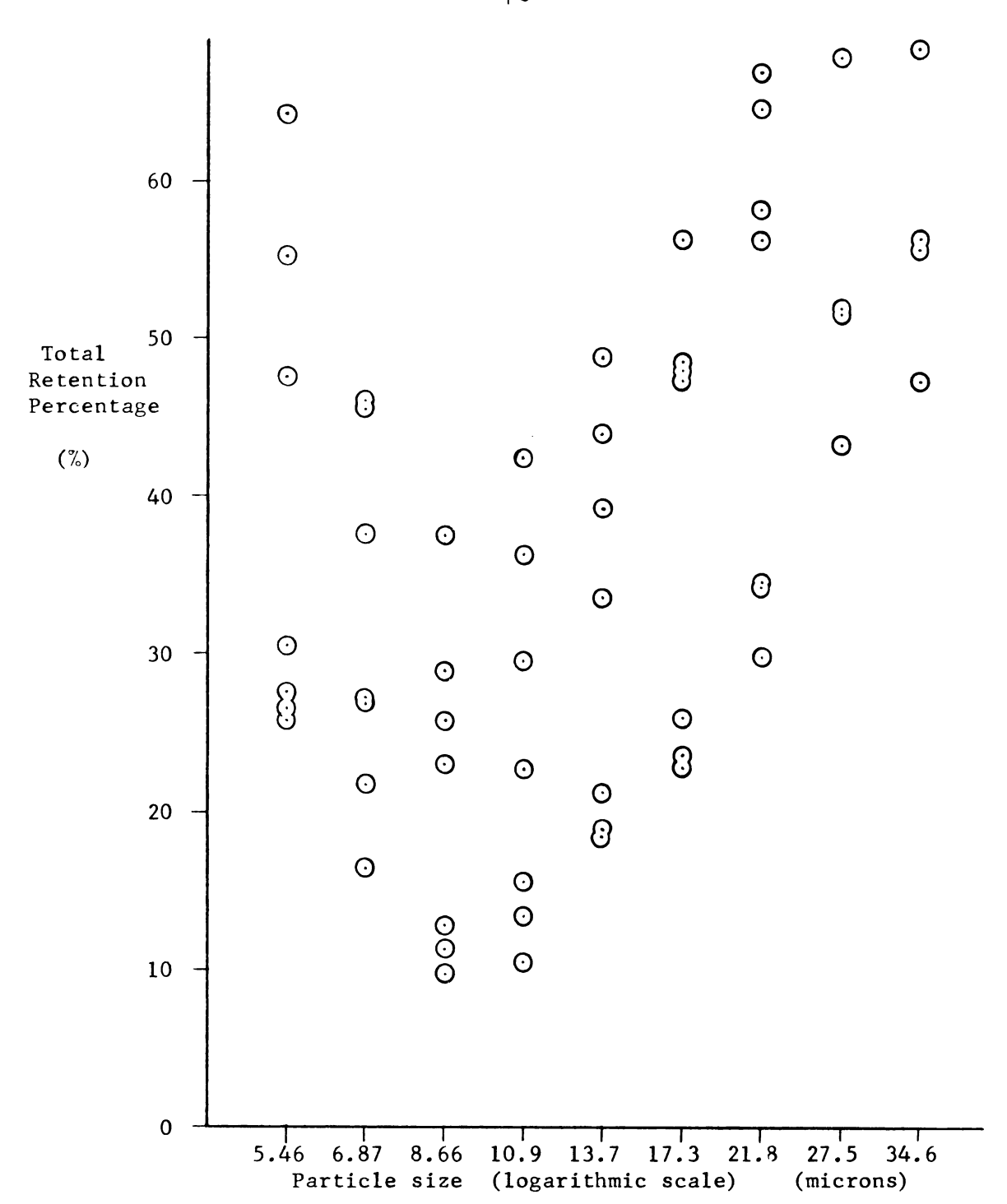


Figure 23. Graph of total retention of particles on glass bed plate. Spread of the data points is probably due to the varying conditions used to obtain the data.

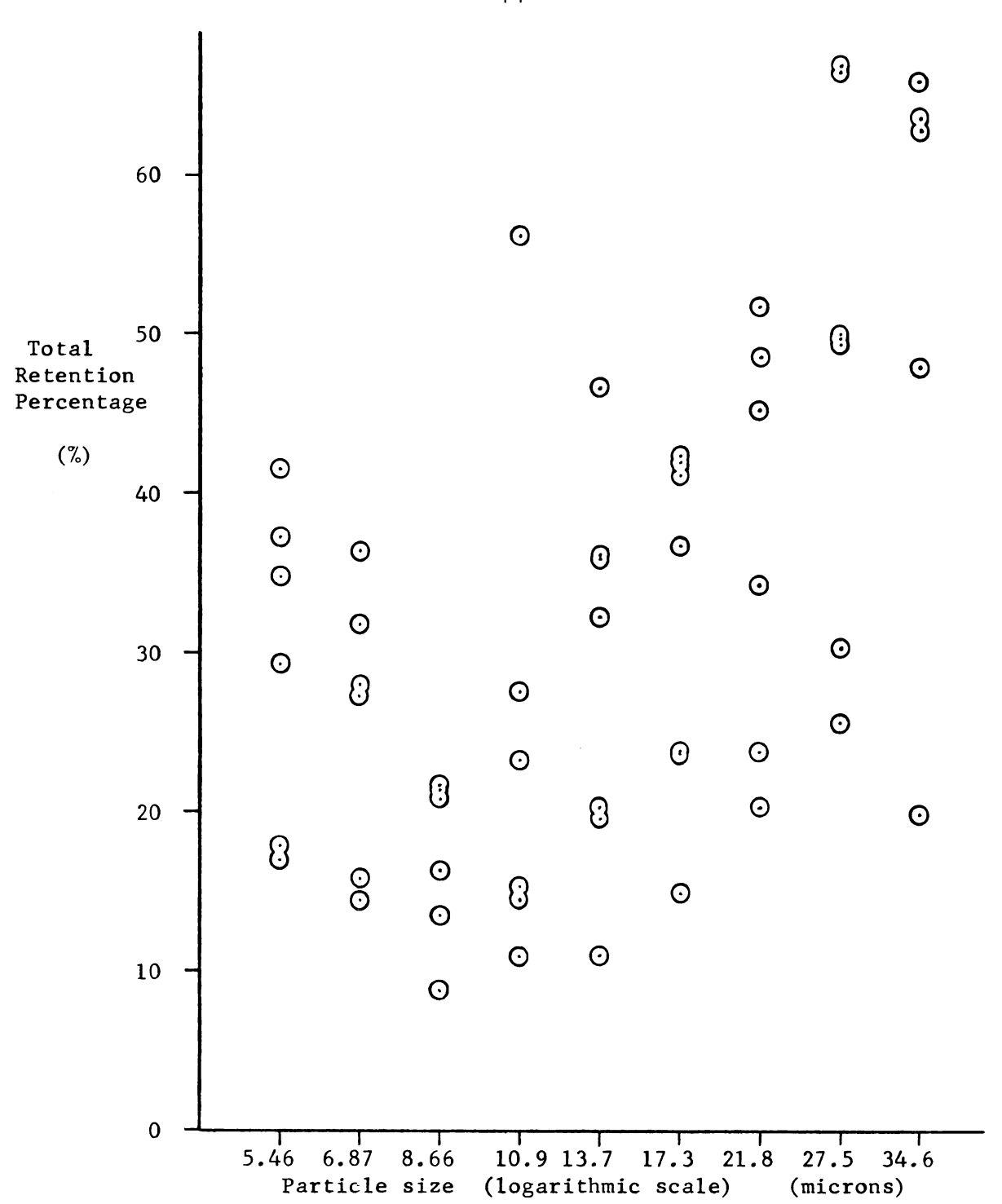


Figure 24. Graph of total retention of particles on 80-grade bed plate. Spread of the data points is probably due to the varying conditions used to obtain the data.

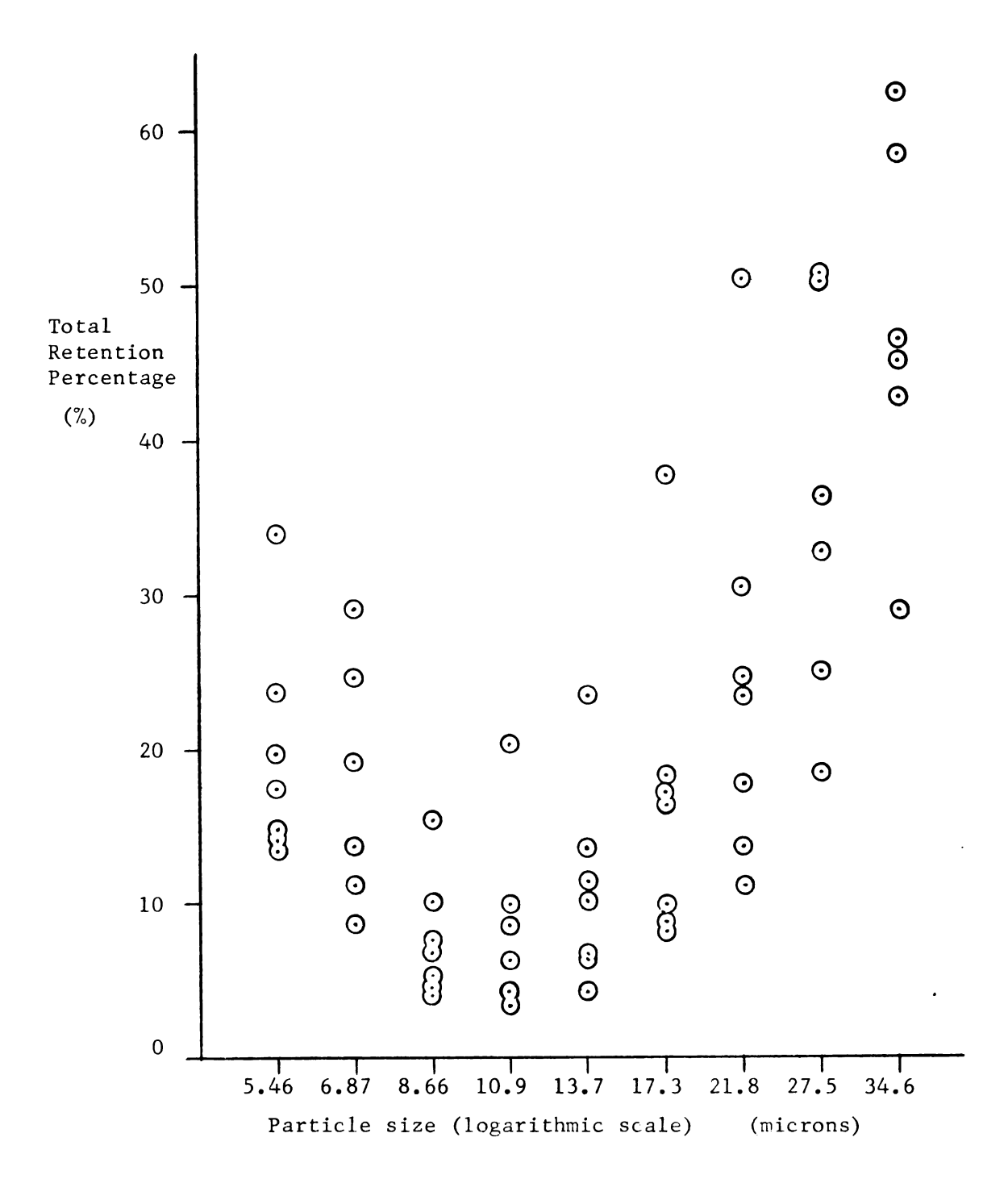


Figure 25. Graph of total retention of particles on 40-grade bed plate. Spread of the data points is probably due to the varying conditions used to obtain the data.

was an attempt to optimize the transport conditions for particles in this size range. However, this was unsuccessful as no improvement in Critical Distance prediction resulted.

The inclusion of model (6), using the "universal velocity profile equations" of Nikuradse (1942), do not add to the understanding of the process, since, on reduction, they yield a value for the Critical Distance X similar in magnitude to those of the other models. The analysis of the relationship between boundary layer conditions and surface roughness is beyond the scope of this study.

Consideration of model (4) shows that it gives the greatest value for the constant K, and therefore the greatest values of Critical Distance X. This might suggest that this concept has some validity for particle transport in thin films of flowing liquid. The "zero net vertical force" approach leads to a question of understanding the situation occurring when a particle is resting on the bed surface and supported by the bed. The vertical force upward, due to the flowing water creating a pressure difference between the upper and lower surfaces of the particle, might be sufficient to induce "saltation." It is suggested that the process of saltation might be the mechanism acting in thin flow which produces the observed effects. Further investigation is necessary to provide the information required to prove or disprove this hypothesis.

SUMMARY AND CONCLUSIONS

Summary

The study was designed to gain knowledge of the intermediate stages of the erosion process by laboratory simulation of thin film transport of eroded material on a watershed. Watershed conditions were simulated and the transport of the silt fraction investigated.

Thin film flow was set up and drops of water containing suspended silt were applied to the surface of the film. When a fixed time had elapsed the flow was stopped and the bed plate removed. After drying, the deposited silt was washed off from sections down the slope. A Coulter Counter was used for sample analysis after the deposited samples had been separated from the bed surface. The use of small amounts of suspended material permitted by application of a Coulter Counter is believed to be the first use of this approach to soil erosion problems.

Various theoretical models were used to predict the distance of transport before deposition of the particles.

Conclusions

The conclusions which were drawn from the study were as follows:

- 1. The Critical Distance of particle transport is independent of particle diameter. The exception to this is the increased distance of transport and reduced total retention of particles with diameters in the range of 8 to 10 microns.
- 2. The Critical Distance X generally decreases as surface roughness increases. However, roughness was not measured quantitatively in this study.
- 3. The Critical Distance X generally increases as bed slope increases. From the theoretical models considered, the Critical Distance X is a function of velocity, which is a function of bed slope.

 Therefore, the Critical Distance is dependent on velocity and bed slope.
- 4. The effect of Stoke's law of settling is masked by some other process for thin film flow. It is suggested that this process might be "saltation."

RECOMMENDATIONS

Further Improvements on the Present Study

The Coulter Counter has shown its usefulness in erosion applications in this study. The instrument provides a method for analyzing small samples with a high degree of accuracy and repeatability. The Coulter Counter has many more apparent uses in erosion studies and these should be investigated thereby taking advantage of the particular qualities of this instrument.

A time-independent method of applying the suspended silt to the flowing water film would facilitate the study of the effects of time on the thin film flow transport process. In this study, the time between application of the silt and cut-off of the water supply was maintained constant (5 seconds). However, the silt application took a finite time, which would complicate a study of time variation, unless an improved method was devised. Also, a method of stopping the flow of water more rapidly would be required to avoid errors due to flow of excess water off the bed plate after cut-off.

A more efficient method of separating the deposited silt material from the bed surface would reduce errors in

total retention percentage and aid in determining the Critical Distance X more accurately.

Recommendations for Further Study

- 1. The present study should be expanded to include an analysis of the boundary layer effects of rough surfaces and the effect of the boundary layer on thin film flow.
- 2. The mechanics of the lift force acting on a particle situated on the bed surface due to flowing liquid is considered to be the most important region of further study. This may lead to a greater understanding of the saltation process.
- 3. A determination of the effect of surface roughness on the velocity profile present in thin film
 flow would greatly assist in these studies. This
 study failed to find a suitable velocity profile
 model which corresponded with the results
 obtained when Stoke's law of settling was assumed
 to apply.
- 4. Field studies are required to relate to the variables involved in laboratory studies of thin film flow to those conditions occurring during runoff on a natural watershed. The lack of suitable field data to use in laboratory simulation studies has been noted elsewhere. Suitable data would simplify thin film flow simulation studies.

5. The study of the effect of rainfall on thin film flow would give further information on the process of overland flow in natural conditions.

REFERENCES

REFERENCES

- Baver, L. D. (1956). <u>Soil Physics</u>. John Wiley and Sons, Incorporated, New York. 489 pp.
- Buckman, H. O., and N. C. Brady (1960). The Nature and Properties of Soils. MacMillan Company, New York. 567 pp.
- Chow, V. T. (1959). Open Channel Hydraulics. McGraw-Hill Book Company, Incorporated, New York. 680 pp.
- Cornell, D. G., and M. J. Pallansch (1966). Counting and Sizing Fat Globules Electronically. Journal of Dairy Science, 49(11), 17-21.
- Einstein, H. A. (1964). River Sedimentation. Section 17-11, pp. 17-35 to 17-67, in V. T. Chow, Ed. <u>Handbook</u> of Applied Hydrology. McGraw-Hill Book Company, Incorporated, New York. 1461 pp.
- Ellison, W. D. (1946). Soil Detachment and Transportation. Soil Conservation, 11(8), 179.
- Ellison, W. D. (1947). Soil Erosion Studies. Agricultural Engineering, 28(4), 145.
- Fulford, G. D. (1964). The Flow of Fluids in Thin Films.

 Pp. 151-236, in T. B. Drew et al. (Ed.) Advances

 in Chemical Engineering, Vol. 5. Academic Press,

 New York. 317 pp.
- Hough, B. K. (1957). <u>Basic Soils Engineering</u>. Ronald Press Company, New York. 513 pp.
- Hudson, N. W. (1963). Raindrop Vize Distribution in High Intensity Storms. Rhodesian Institution of Agricultural Research, 1(1), 6-11.
- Hudson, N. W. (1964). A Review of Artificial Rainfall Simulators. Rhodesian Department of Conservation and Extension Research Bulletin, No. 7.
- Kalinske, A. A. (1942). Criteria for Determining Sand Transport by Surface Creep and Saltation. Transactions of the American Geophysical Union, 23, 639-643.

- Kalinske, A. A. (1947). Movement of Sediment as Bed in Rivers. Transactions of the American Geophysical Union, 28, 615-620.
- Mavis, F. T. (1935). The Transport of Detritus by Flowing Water. State University of Iowa Studies in Engineering Bulletin, No. 5.
- Meyer, L. D., and D. L. McCune (1958). Rainfall Simulator for Runoff Plots. Agricultural Engineering, 39(10), 644-646.
- Meyer, L. D. (1965). Symposium on Simulation of Rainfall for Soil Erosion Research. Transactions of the American Society of Agricultural Engineering, 8(1), 63-75.
- Meyer, L. D., and E. J. Monke (1965). Mechanics of Soil Erosion by Rainfall and Overland Flow. Transactions of the American Society of Agricultural Engineering, 8(4). 572-580.
- Mutchler, C. K. (1967). Parameters for Describing Raindrop Splash. Journal of Soil and Water Conservation, May-June, 1967.
- Nikuradse, J. (1942). <u>Turbulente Reibungsschichten an der</u> Platte. Z.W.B., R. Oldenbourg, Munchen, Germany.
- Osborn, B. (1955). How Rainfall and Runoff Erode Soil.

 Pp. 126-135, in A. Stefferund (Ed.) The Yearbook of Agriculture 1955-Water. United States Printing Office. 751 pp.
- Palmer, R. S. (1965). Waterdrop Impact Forces. Transactions of the American Society of Agricultural Engineering, 8(1), 70-71.
- Raudkivi, A. J. (1967). Locse Boundary Hydraulics. Pergamon Press, London, 331 pp.
- Rose, C. W. (1960). Soil Detachment Caused by Rainfall. Soil Science, 89(1), 28-30.
- Schlichting, H. (1968). <u>Boundary Layer Theory</u>. McGraw-Hill Book Company, <u>Incorporated</u>, New York. 317 pp.
- Schwab, G. O., R. K. Frevert, T. W. Edminster, and K. K. Barnes (1966). Soil and Water Conservation Engineering. John Wiley and Sons, New York. 683 pp.

- Streeter, V. L. (1968). Fluid Mechanics. McGraw-Hill Book Company, Incorporated, New York. 480 pp.
- Webster's Seventh New Collegiate Dictionary (1961).

 G. and C. Merriam Company, Springfield, Massachusetts. 1174 pp.

APPENDICES

APPENDIX A

CALIBRATION AND USE OF THE
COULTER COUNTER

APPENDIX A

CALIBRATION AND USE OF THE COULTER COUNTER

Model B, which is shown in Figure 8. The components of the Coulter Counter are given diagramatically in Figure 26.

The instrument determines the number and size of the particles in suspension in an electrically conductive liquid by drawing the suspension through a small aperture and monitoring the change in conductivity between two electrodes, one placed in the liquid on either side of the aperture.

The passage of a particle through the aperture causes an increase in the resistance between the two electrodes which produces a pulse signal whose magnitude is proportional to the particle volume. In the analysis of a sample the pulses are scaled and counted electronically.

The manometer unit indicated in the diagram consists of a mercury manometer and reservoir connected to a vacuum source. The open end of the manometer is provided with a glass tube of known internal diameter. By sealing electrical contacts into the walls of the tube at known intervals the volume of mercury passing the contacts is known. These contacts are used to trigger and stop the electrical counter unit.

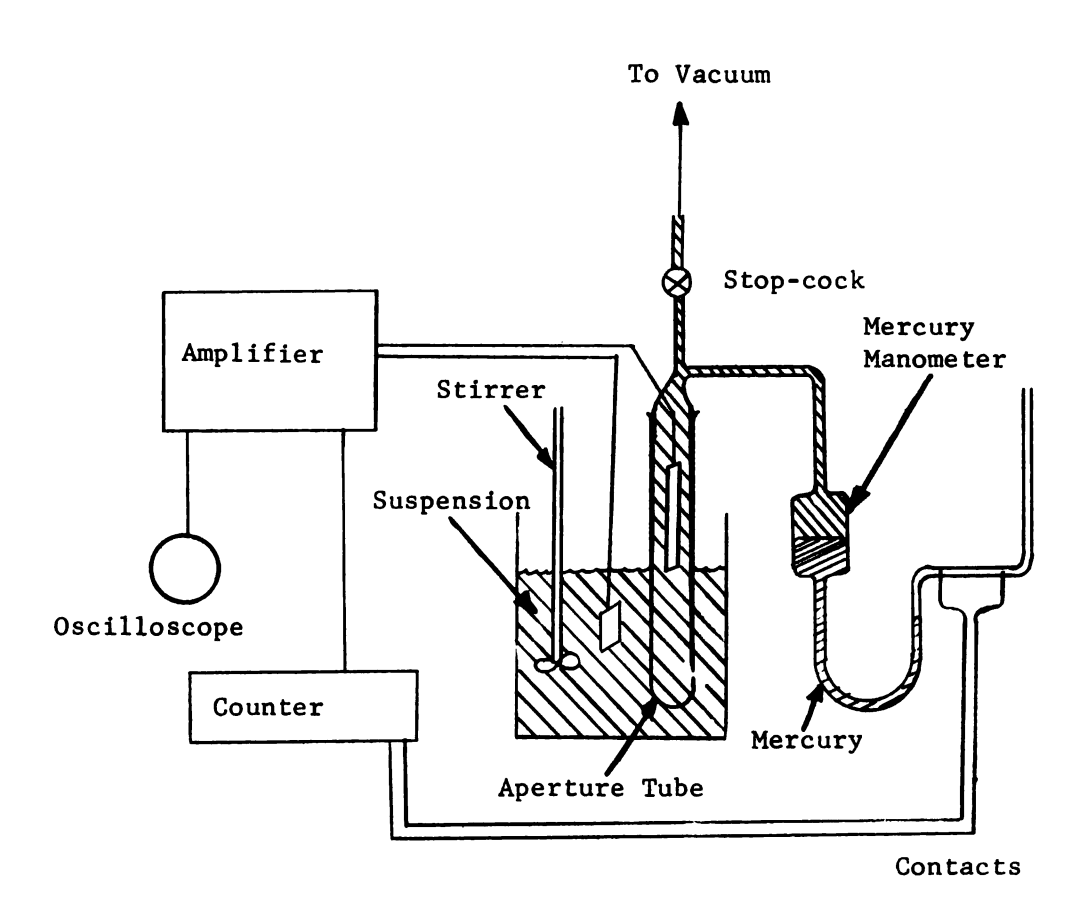


Figure 26. Diagram of the Coulter Counter.

The end of the manometer under vacuum is also attached to the aperture element and the whole space is filled with the same electrolyte as used for the sample. The electrolyte solution used was a 2% potassium chloride solution as recommended by Cornell and Pallansch (1966). The solution was made with distilled water and filtered through 12 micron, 1.4 micron, and 0.8 micron Millepore filters under vacuum. The typical particle count of this solution is given in Appendix C and the various batches used during testing showed little variation from this. The background counts obtained from the blank solutions showed that correction of the particle counts obtained were not necessary.

When the manameter is connected to the vacuum, the mercury rises into the reservoir. On closing the valve the mercury falls under gravity drawing the sample through the aperture. As the mercury passes the electrical contacts the counter is switched on, the pulses are monitored, and the counter is switched off. In this study, the aperture tube was a #17005 manufactured by Coulter Electronics Incorporated with an aperture diameter of 100 microns. The volume of sample drawn in for each test was set at 500 microliters.

In order to obtain a particle size analysis, the pulses obtained were amplified and compared to a preset threshold value. If the pulse exceed this value it was

registered on the counter. By varying the threshold value and increasing the amplification of the incoming signals in known steps, a particle size distribution was calculated.

The instrument was found to be particularly susceptable to electrical noise. A location was found where electrical noise was low. The power supply to the instrument was fed through a Sola transformer to eliminate irregularities in the supply voltage. However, the visible output on the oscilloscope was continually monitored for signs of electrical interference. If interference was observed during a test, the test was repeated. In addition, the aperture quickly became blocked when dust or foreign matter was present in the sample. Great care was necessary to exclude foreign matter from the samples by keeping them covered at all times. The aperture was watched by means of a small microscope (35 power) provided for this purpose. If the aperture became blocked during a test, the test was repeated after cleaning the aperture with a small, short-bristled brush. Care was taken to avoid damage of the delicate aperture.

Calibration

The material used for calibration was a suspension of styrene divinylbenzene copolymer latex, manufactured by the Dow Chemical Company and having a size range of 6 to 14 microns diameter. This suspension was examined under an optical microscope and the particle diameters measured.

From this it was determined that the particles in suspension were in three separate size ranges: (1) 6 to 8 microns (this class had the greatest variation); (2) 10 to 11 microns, and (3) 14 microns (this class had the least variation). By measuring the diameters of several hundred particles it was possible to determine that the third size range had a mean diameter of 14.0 (±0.25) microns. These particles fulfill the condition stated by the manufacturer that the optimum size to use for calibration is between 5 and 20 per cent of the aperture diameter—in this case, between 5 and 20 microns. It was also noted that all the particles were smooth and approximately spherical.

The calibration procedure was as follows:

- One drop of the suspension was added to 125 ml. of the potassium chloride solution in a 250 ml. beaker. A standard eye-dropper was used for this.
- 2. The suspension was placed under the aperture and the stirrer and electrodes positioned.
- 3. The beaker was raised so that the aperture became immersed in the suspension.
- 4. The stirrer was started and the speed of rotation established so that maximum suspension was maintained without violent agitation causing errors due to air bubble entrainment.

7	

- 5. The counter was reset so that the pulses could be observed on the oscilloscope and the amplification was adjusted until the peaks due to the 14 micron particles corresponded to a threshold value of between 15 and 30 on the threshold dial. The threshold value was noted.
- 6. The threshold was set at half of this observed pulse height level and several counts taken. The average full count n_f was then calculated.
- 7. The threshold was set at about $1\frac{1}{2}$ times the cbserved pulse height and several oversize particle counts were taken and averaged to find the oversize count: n_0
- 8. The half count is calculated using the formula:

$$n_{m} = \frac{1}{2}(n_{f} + n_{O})$$

- 9. By trial and error, the threshold was adjusted until the setting gave the half count value n_m . The values of the threshold t_L , amplification A, and aperture current I are recorded.
- 10. The calibration constant is calculated using formula:

$$h = \frac{v_L}{IAt_L}$$

where \mathbf{v}_{L} = the volume of monc-sized particles in cubic microns.

(For 14 micron diameter particles, v_L = 1437 cubic microns.)

Sample Analysis

According to the U. S. Bureau of Soil Systems (Baver, 1956, p. 16) silt particles have a size range of 5 to 50 microns. The aperture current and amplification settings were used to analyze this size range using the calibration constant. The formulae were:

$$v_L = ht_L IA$$

$$d_{L} = 1.241 \sqrt[3]{V_{L}}$$

where d_L = diameter of the smallest particle counted.

To cover the size range indicated, the values of the settings used were:

Threshold $t_{L} = 40, 20$

Aperture current I = 8, 4, 2, 1

Amplification A = 64, 32, 16, 8, 4, 2, 1, $\frac{1}{2}$.

However, for the silt sample used, the particles were in the range of 5 to 44 microns and hence the value $t_{\rm L}$ = 40 was not used. For settings $t_{\rm L}$ = 20, I = 8, A = 64 a zero count was obtained in all cases.

For the analysis of samples, the procedure as given below was:

- 1. The beaker containing the sample suspended in 125 ml. of KCl solution was placed under the aperture tube. The beaker was then raised to immerse the aperture tube in the suspension so that the aperture was about 1 cm. from the bottom and side of the beaker. The aperture was placed close to the side of the beaker so that the aperture can be seen through the microscope.
- 2. The stirrer was adjusted to give maximum suspension without causing air bubble entrainment.
- 3. The counter controls were set as follows:

$$t_{I} = 20$$
, $I = 4$, $A = 64$

- 4. The vacuum stopcock was opened to lower the mercury column below the start control contact.
- 5. The beaker was retated about 45° before each test to resuspend sample material which had been deposited in the less turbulent region under the aperture tube. This ensured more uniform counts (x_1, x_2, x_3, x_4) .
- 6. The counter was zeroed and reset to avoid polarization of the electrodes.

- 7. The aperture was checked visually for freedom from blockage and the vacuum stopcock closed. This released the mercury and drew the sample through the aperture.
- 8. After the counter had registered a count, it was noted and the test was repeated a total of four times per setting.
- 9. The counter controls were reset, first reducing stepwise the aperture current I, and when its minimum value was reached then the amplification A. A run of four tests was performed for each setting and the values for the counter controls t_L , I, A and the counts were noted on a data sheet (see Table 4).
- *10. The data processed as indicated in the Data Analysis section.

Appendix A is modelled on "Instruction Manual," Coulter Counter Industrial Model B, Coulter Electronics Industrial Division, 2525 North Sheffield Avenue, Chicago, Illinois, 60614, which contains an extensive technical bibliography.

APPENDIX B

PRELIMINARY LENGTH OF BED SLOPE CALCULATION

APPENDIX B

PRELIMINARY LENGTH OF BED SLOPE CALCULATION

The conditions considered are extremes in order that all eventualities might be taken into account during experimentation.

Consider a flow depth of 0.5 cm. with a velocity of 25.0 cm./sec. Assume that the velocity profile is constant velocity with depth with a sharp reduction to zero close to bed surface. This is a necessary oversimplification at this stage.

Consider a particle of 4 microns diameter which is smaller than those in the silt range, according to the U.S. Bureau of Scils System (Baver, 1956, p. 16). From Stoke's law the terminal velocity of settling is given as:

$$v_s = \frac{2}{9} \frac{(d_s - d) gr^2}{\mu}$$
 (B.1)

For silt, which is predominantly quartz (Buckman and Brady (1960, p. 176), Baver (1956) quotes quartz as having a density of 2.50 to 2.80 gm./cm.³ and suggests an average value of 2.65 gm./cm.³ This average value was used in all calculations.

A water temperature of 10°C was used in this calculation. This temperature gives the following:

Viscosity of water at $10^{\circ}\text{C} = \mu = 1.32 \text{ x } 10^{-5} \text{ gm./cm. sec.}$ Density of water at $10^{\circ}\text{C} = d = 1.00 \text{ gm./cm.}^3$

These values were slightly lower than those expected to be encountered in testing.

Then in equation (B.1):

$$v_s = \frac{2}{9} \frac{(2.65 - 1.00) \times 980 \times (2 \times 10^{-4})^2}{1.32 \times 10^{-5}}$$

= 1.09 cm./sec.

Therefore time taken to fall 0.5 cm.

$$t = \frac{0.5}{1.09} = 0.46 \text{ sec.}$$

During this time, the particle is transported by the flowing water.

Distance transported = $s = 0.46 \times 25$

$$= 11.5 \text{ cm}.$$

This indicates that even under extreme conditions the distance which the particle will be expected to move will be of the order of 10 cm. This was confirmed by preliminary testing. To allow for non-uniform end conditions, a length of 60 cm. was chosen.

APPENDIX C

DATA

Analysis of Typical
Blank 2% Potassium Chloride
Solution

t_	-	۸	Raw Counts				
t _L	I	A —	* ₁	* ₂	x 3	*4	*4
							_
20	4	64	1	1	1	1	
20	2	64	1	1	1	1	
20	1	64	1	2	1	2	
20	1	32	2	1	2	2	
20	1	16	2	2	2	1	
20	1	8	2	1	2	2	
20	1	4	2	2	2 .	2	
20	1	2	6	5	8	7	
20	1	1	17	20	16	17	
20	1	1/2	36	39	30	56	



Slope: 3%

Surface: 80-Grade

Master Silt Analysis

	-		R	Raw Counts		
t _L	I	Α	×I	*2	x 3	*4
20	4	64	14	15	16	11
20	2	64	83	66	96	82
20	1	64	367	348	342	367
20	1	32	978	932	951	950
20	1	16	1796	1741	1880	1816
20	1	8	2717	2712	2806	2816
20	1	4	3659	3654	3616	3576
20	1	2	4452	4510	4498	4526
20	1	1	5302	5185	5320	5251
20	1	1/2	6850	6873	6794	6803



Slope: 3% Surface: 80-Grade

Distance down slope: 0.64 cm

t_				Raw C	Counts		
^t L	t _L I	Α -	* ₁	* ₂	х 3	*4	
							_
20	4	64	1	2	3	2	
20	2	64	6	4	5	8	
20	1	64	41	30	34	29	
20	1	32	60	77	71	71	
20	1	16	119	118	122	107	
20	1	8	148	164	149	138	
20	1	4	229	197	209	185	
20	1	2	239	226	224	222	
20	1	1	353	287	296	289	
20	1	1/2	514	456	495	479	

		}
		<i>\\ \\ \\ \\ \\ \\ \\ \\</i>
		Ì

Slope: 3% Surface: 80-Grade

Distance down slope: 2.54 cm

	_		Raw Counts				
t _L	I	A —	* ₁	*2	x 3	* ₄	
20	4	64	14	10	18	16	
20	2	64	88	106	89	95	
20	1	64	303	310	317	313	
20	1	32	620	581	659	628	
20	1	16	976	912	931	932	
20	1	8	1167	1158	1202	1203	
20	1	4	1425	1393	1376	1386	
20	1 .	2	1548	1671	1532	1505	
20	1	1	1835	1840	1804	1766	
20	1	1/2	2382	2415	2171	1949	



Slope: 3% Surface: 80-Grade

Distance down slope: 5.08 cm

t	T	Α	Raw Counts			
t _L	I	A —	× ₁	* ₂	*3	* ₄
20	4	64	7	15	20	9
20	2	64	84	69	72	78
20	1	64	228	230	233	225
20	1	32	422	457	470	477
20	1	16	781	710	699	721
20	1	8	986	875	958	944
20	1	4	1071	1092	1108	1102
20	1	2	1274	1217	1258	1196
20	1	1	1492	1428	1500	1440
20	1	1/2	1934	1877	1957	1985

Slope: 3% Surface: 80-Grade

Distance down slope: 7.62 cm

	t.	I	Α	Raw Counts					
_	^t L	<u> </u>	л <u> </u>	× ₁	*2	^x 3	*4		
-									
	20	4	64	14	7	14	17		
	20	2	64	78	63	78 ^	64		
	20	1	64	240	231	216	210		
	20	1	32	425	447	434	399		
	20	1	16	624	598	602	602		
	20	1	8	747	793	792	714		
	20	1	4	894	880	877	879		
	20	1	2	1055	1075	959	949		
	20	1	1	1115	1201	1150	1161		
	20	1	1/2	1635	1511	1472	1504		

Slope: 3% Surface: 80-Grade

Distance down slope: 10.16 cm

t.	I A		Raw Counts				
t _L	Ι	•	× ₁	× ₂	*3	*4	
20	4	64	8	4	6	2	
20	2	64	40	33	37	39	
20	1	64	102	108	86	98	
20	1	32	212	208	195	212	
20	1	16	320	328	298	314	
20	1	8	415	401	431	417	
20	1	4	507	487	505	467	
20	1	2	578	575	595	545	
20	1	1	713	625	866	666	
20	1	1/2	926	936	894	876	

Slope: 3% Surface: 80-Grade

Distance down slope: 12.70 cm

^t L	I	Α	Raw Counts				
L	_	Α	*1	* ₂	*3	×4	
20	4	64	5	8	4	5	
20	2	64	47	38	35	34	
20	1	64	144	139	158	139	
20	1	32	267	280	265	244	
20	1	16	425	415	427	418	
20	1	8	534	511	532	542	
20	1	4	629	640	632	649	
20	1	2	719	722	722	722	
20	1	1	829	839	838	876	
20	1	1/2	1217	1167	1175	1196	

Slope: 3% Surface: 80-Grade

Distance down slope: 15.24 cm

t.	т	Α		Raw Co	ounts	
t _L	I	A	x 1	* ₂	x 3	* ₄
20	4	64	4	6	9	6
20	2	64	32	43	37	34
20	1	64	91	98	99	102
20	1	32	220	229	219	210
20	1	16	330	361	352	310
20	1	8	415	468	432	446
20	1	4	532	578	572	571
20	1	2	658	650	660	626
20	1	1	830	781	822	816
20	1	1/2	1188	1229	1184	1116

Slope: 3% Surface: 80-Grade

Distance down slope: 17.78 cm

^t L	I	Α _	т Δ		Raw Counts				
	1	-	x ₁	* ₂	* ₃	×4	_		
							=		
20	4	64	7	6	2	7			
20	2	64	36	21	26	37			
20	1	64	74	83	71	88			
20	1	32	144	149	148	151			
20	1	16	227	225	240	222			
20	1	8	318	304	310	306			
20	1	4	385	394	382	394			
20	1	2	436	438	420	484			
20	1	1	492	567	541	472			
20	1	1/2	809	821	817	862			

Run No: 3 Surface: Glass Slope: 5%

Mean Flow Velocity: 22.9 cm/sec Temperature: 13.9 °C

Mean Flow Depth: 0.14 cm

near New Country											
Particle Diameter (Microns)	5.46	6.87	8.66	10.9	13.7	17.3	21.8	27.5	34.6		
Mean Master Count	29168	15550	12213 .	14938	14463	12900	9350	5478	2078		
Distance Down Slope (cm)	e										
5.08	1098	433	363	377	595	773	687	263	31		
7.62	1314	587	275	507	691	823	933	534	141		
10.16	2041	917	568	692	958	1186	1406	968	377		
12.70	1944	959	593	608	1099	1225	995	1194	377		
15.24	1084	541	324	276	602	747	741	491	211		
17.78					712	566	652	381	148		
20.32	850	374	359	473	531	404	322	199	71		
22.86	557	400	327	468	461	367	307	178	62		
Total % Retained	30.46	27.08	23.00	22.76	39.05	47.21	64.63	76.82	68.23		
Critical Distance (cm)	10.16	12.70	12.70	10.16	12.70	12.70	10.16	12.50	11.43		

Run No: 4 Surface: Glass Slope: 5%

Mean Flow Velocity: 16.0 cm/sec Temperature: 14.2 °C

Mean Flow Depth: 0.11 cm

Particle Diameter (Microns)	5.46	6.87	8.66	10.9	13.7	17.3	21.8	27.5	34.6
Mean Master Count	17723	11643	19580	19535	19285	16305	10455	4658	1865
Distance Down Slop (cm)	e								
5.08	948	350	308	612	895	877	705	292	58
7.62	2023	1055	550	1043	1383	1590	1327	841	329
10.16	2361	1392	897	1305	1773	1943	1612	1033	430
12.70	1874	792	801	1118	1483	1341	1000	545	205
15.24	1018	418	600	770	851	677	437	207	74
17.78	1043	502	553	824	741	545	360	173	63
20.32	1204	477	786	871	836	620	365	183	68
22.86	908	368	535	526	528	318	264	117	45
Total % Retained	64.19	45.99	25.67	36.18	43.97	48.51	58.05	72.79	68.21
Critical Distance (cm)	10.16	10.16	10.16	10.16	10.16	10.16	10.16	10.16	10.16

Run No: 6 Surface: Glass Slope: 1%

Mean Flow Velocity: 13.7 cm/sec Temperature: 12.8 °C

Mean Flow Depth: 0.21 cm

Particle Diameter (Microns)	5.46	6.87	8.66	10.9	13.7	17.3	21.8	27.5	34.6
Mean Master Count	14953	7875	8305	10053	11393	9168	6945	3175	993
Distance Down Slop (cm)	e								
0.64	250	62	86	59	112	121	113	63	14
2.54	1489	506	372	449	679	918	943	617	253
5.08	1379	542	479	476	776	993	969	586	232
7.62	1187	513	294	584	733	857	716	362	111
10.16	855	247	201	316	437	468	419	205	64
12.70	593	292	233	287	367	313	263	101	36
15.24	320	228	193	224	185	235	118	67	27
17.78	487	231	280	235	286	227	188	83	32
20.32	302	221	166	217	181	179	126	50	14
22.86	231	107	103	113	75	81	47	21	6
Total % Retained	47.45	37.462	8.99	29.44	33.62	47.89	56.19	67.86	79.40
Critical Distance (cm)	2.54	5.08	5.08	7.62	5.08	5.08	5.08	2.54	2.54

Run No: 8 Surface: Glass Slope: 1%

Mean Flow Velocity: 10.2cm/sec Temperature: 12.8 °C

Mean Flow Depth: 0.18 cm

Particle Diameter (Microns)	5.46	6.87	8.66	10.9	13.7	17.3	21.8	27.5	34.6
Mean Master Count	19180	10895	12165	14708	13623	11863	7860	3720	1135
Distance Down Slope (cm)	e								
0.64	917	290	342	374	481	503	497	255	88
2.54	2398	959	831 .	955.	1400	1685	1664	1017	399
5.08	2361	1206	710	1389	1490	1766	1366	749	276
7.62	1534	972	776	1150	1217	1123	772	345	121
10.16.	1299	540	634	789	789	664	425	174	61
12.70	627	310	346	471	454	346	187	93	27
15.24	481	265	302	356.	346	245	136	48	25
17.78	409	207	351	363.	303	199	128	61	17
20.32	359	210	261	269	178	143	81	50	17
Total % Retained	55.14	45.52	37.43	42.30	48.87	56.06	66.87	74.24	90.83
Critical Distance (cm)	2.54	5.08	2.54	5.08	5.08	5.08	2.54	2.54	2.54

Run No: 9 Surface: 80-Grade Slope: 5%

Mean Flow Velocity: 14.5 cm/sec Temperature: 12.8 °C

Mean Flow Depth: .16 cm

			Me	ean Raw	Counts				
Particle Diameter (Microns)	5.46	6.87	8.66	10.9	13.7	17.3	21.8	27.5	34.6
Mean Master Count	9223	2735	2138	3538	5275	6738	5600	3233	875
Distance Down Slope (cm)	e								
0.64				48	54	45	52	38	17
2.54				245	320	437	418	289	112
5.08				216	352	462	463	311	117
7.62				343	451	604	534	319	116
10.16				278	325	382	347	205	68
12.70				250	259	271	250	156	52
15.24				305	244	244	191	108	40
17.78				122	158	148	109	63	20
20.32				56	207	157	102	77	23
22.86				124	83	88	66	42	11
Total % Retained				56.16	46.50	42.13	45.21	49.74	65.83
Critical Distance (cm)				7.62	7.62	7.62	7.62	7.62	5.08

Run No: 10 Surface: 80-Grade Slope: 1%

Mean Flow Velocity: 12.0 cm/sec Temperature: 11.7 °C

Mean Flow Depth: 0.27cm

Particle Diameter (Microns)	546	6.87	8.66	10.9	13.7	17.3	21.8	27.5	34.6
Mean Master Count	17320	8873	10085	12813	11525	10593	7633	3518	1048
Distance Down Slope (cm)	e								
0.64	3.6	134	59	83	108	109	146	90	32
2.54	1493	604	255	677	777	946	856	597	228
5.08	1316	486	365	623	715	756	710	413	146
7.62	930	632	427	595	683	678	639	355	139
10.16	655	249	305	233	436	391	347	195	69
12.70	759	299	253	391	473	464	417	261	97
15.24	402	246	127	244	275	283	260	157	52
17.78	502	201	175	210	272	288	219	122	39
20.32	484	242	146	286	227	262	193	99	32
22.80	346	126	82	172	182	166	163	65	30
Total % Retained	41.59	36.28	21.76	27.43	35.99	41.00	51.75	66.91	82.44
Critical Distance (cm)	2.54	7.62	7.62	2.54	2.54	2.54	2.54	2.54	2.54

Run No: 11 Surface: 80-Grade Slope 5%

Mean Flow Velocity: 11.7 cm/sec Temperature: 11.7 °C

Mean Flow Depth: 0.15 cm

Particle Diameter (Microns)	5.46	6.87	8.66	10.9	13.7	17.3	21.8	27.5	34.6
Mean Master Count	17883	7915	8738	10110	9635	9095	6458	3348	790
Distance Down Slop (cm)	e								
0.64	115	99	57	48	89	87	82	43	13
2.54	527	243	177	205	342	412	406	244	59
5.08	877	237	226	277	421	441	506	312	125
7.62	743	379	399	377	607	662	595	365	144
10.16	749	316	256	407	417	553	403	243	99
12.70	647	210	186	232	377	343	270	161	57
15.24	516	203	181	266	271	315	215	108	46
17.78	389	169	122	207	237	192	204	77	35
20.32	335	204	165	149	176	200	138	75	29
22.86	294	153	86	161	171	129	97	45	21
Total % Retained	29.03	27.96	21.23	23.04	32.19	36.66	45.15	49.97	63.43
Critical Distance (cm)	5.08	7.62	7.62	10.16	7.62	7.62	7.62	7.62	7.62

Run No: 12 Surface: 80-Grade Slope: 1%

Mean Flow Velocity: 7.6 cm/sec Temperature: 11.7 °C

Mean Flow Depth: 0.21 cm

Particle Diameter (Microns)	5.46	6.87	8.66	10.9	13.7	17.3	21.8	27.5	34.6
Mean Master Count	16605	9185	10110	10793	10958	9373	6518	2765	675
Distance Down Slope (cm)	e								
0.64	751	423	306	251	447	470	475	290	123
2.54	2238	983	384	861	1180	1328	1208	828	296
5.08	1219	601	437	666	925	934	711	358	113
7.62	736	359	290	451	543	515	322	173	42
10.16	467	199	277	322	418	308	211	76	20
12.70	488	248	282	279	329	270	169	85	24
15.24	269	101	127	245	116	104	61	26	15
Total % Retained	37.15	31.73	20.80	27.56	36.12	41.92	48.44	66.40	93.73
Critical Distance (cm)	2.54	2.54	5.08	2.54	2.54	2.54	2.54	2.54	2.54

Run No: 13 Surface: 80-Grade Slope: 3%

Mean Flow Velocity: 16.2 cm/sec Temperature: 11.7 °C

Mean Flow Depth: 0.20 cm

			M	ean Raw	Counts				
Particle Diameter (Microns)	5.46	6.87	8.66	10.9	13.7	17.3	21.8	27.5	34.6
Mean Master Count	15655	7680	8703	8635	9545	8555	5968	2743	678
Distance Down Slope (cm)	e								
0.64	180	79	23	55	33	47	36	28	4
2.54	418	247	169	213	245	316	311	216	80
5.08	473	229	143	153	213	271	228	153	63
7.62	374	147	127	121	155	180	202	154	58
10.16	191	144	82	76	101	108	108	61	32
12.70	343	124	84	108	109	157	119	107	33
15.24	367	164	85	123	102	119	122	61	30
17.78	309	74	56	79	81	81	69	49	25
Total % Retained	16.96	15.73	8.84	10.75	10.89	14.95	20.02	30.22	47.94
Critical Distance (cm)	5.08	2.54	2.54	2.54	2.54	2.54	2.54	2.54	2.54

Run No: 14 Surface: 80-Grade Slope: 3%

Mean Flow Velocity: 10.9 cm/sec Temperature: 10.8 °C

Mean Flow Depth: .17 cm

Hean Flow	Deptii.	• 17 CI	11						
			Me	ean Raw	Counts				
Particle Diameter (Microns)	546	6.87	8.66	10.9	13.7	17.3	21.8	27.5	34.6
Distance Down Slope (cm)	e								
0.64	184	35	52	32	82	87	84	32	8.
2.54	1840	603	337	462	896	1391	1415	869	250
5.08	1217	476	386	536	679	949	896	642	295
7.62	1117	411	424	492	766	812	703	442	161
10.16	480	180	193	252	270	308	247	157	56
12.70	492	252	228	247	293	285	239	152	41
15.24	291	163	80	1.02	131	195	69	79	38
17.78	212	69	85	68	76	89	92	63	28
Total % Retained	17.85	14.35	13.59	16.22	20.22	23.90	23.77	25.67	19.78
Critical Distance (cm)	2.54	2.54	7.62	5.08	2.54	2.54	2.54	2.54	5.08

Run No: 15 Surface: Glass Slope 3%

Mean Flow Velocity: 16.4 cm/sec Temperature: 11.1 °C

Mean Flow Depth: 0.15 cm

				nean R	aw coun				
Particle Diameter (Microns)	5.46	6.87	8.66	10.9	13.7	17.3	21.8	27.5	34.6
Mean Master Count	10080	6535	5608	6948	6388	5468	4160	1698	553
Distance Down Slop (cm)	e								
508	328	123	66	120	127	177	146	51	8
7.62	33.6	190	146	96	209	318	341	197	53
10.16	445	193	127	116	250	232	245	149	63
12.70	601	134	57	69	189	162	125	100	47
15.24	261	116	98	77	122	119	105	67	26
17.78	252	94	95	63	102	91	95	61	22
20.32	303	114	54	95	117	88	104	54	20
22.86	252	103	76	82	56	105	75	52	22
Total % Retained	27.56	16.33	12.82	10.33	18.35	23.63	29.71	43.05	47.20
Critical Distance (cm)	12.70	10.16	10.16	5.08	10.16	7.62	7.62	7.62	10.16

Run No: 16 Surface: Glass Slope: 3%

Mean Flow Velocity: 12.8 cm/sec Temperature: 11.1 °C

Mean Flow Depth: 0.14 cm

	Heal Naw Counts									
Particle Diameter (Microns)	5.46	6.87	8.66	10.9	13.7	17.3	21.8	27.5	34.6	
Mean Master Count	9223	4013	5153	4573	5158	5665	4328	1935	685	
Distance Down Slope (cm)										
2.54	95	22	24	11	20	26	20	6	1	
5.08	310	184	60	47	98	175	267	172	44	
7.62	498	324	61	164	230	365	423	317	120	
10.61	512	166	118	154	225	243	314	199	101	
12.70	287	71	69	118	140	138	158	112	40	
15.24	218	77	51	105	110	120	120	68	35	
17.78	234	128	61	36	93	107	81	62	20	
20.32	217	98	60	68	117	112	92	67	24	
Total %	25.70	26.67	9.77	15.39	20.11	22.71	34.08	51.82	56.20	
Critical Distance (cm)	10.16	7.62	10.16	7.62	7.62	7.62	7.62	7.62	7.62	

Run No: 17 Surface: 40-Grade Slope: 5%

Mean Flow Velocity: 13.2 cm/sec Temperature: 11.1 °C

Mean Flow Depth: .21 cm

Particle Diameter (Microns)	5.46	6.87	8.66	10.9	13.7	17.3	21.8	27.5	34.6
Mean Master Count	10828	4508	6185	6025	5643	5055	3678	1885	493
Distance Down Slope (cm)	e								
0.64	407	165	92	69	69	200	173	141	7 5
2.54	262	114	33	49	44	64	120	99	53
5.08	293	118	44	52	51	74	82	116	38
7.62	279	124	64	67	30	94	81	71	31
10.16	226	94	52	31	46	76	50	46	14

Total % Retained	13.55	13.64	4.61	4.45	4.25	10.05	13.76	25.09	42.80
Critical Distance (cm)	0.64	0.64	0.64	0.64	0.64	0.64	0.64	0.64	0.64

Run No: 18 Surface: 40-Grade Slope: 5%

Mean Flow Velocity: 10.2 cm/sec Temperature: 11.1°C

Mean Flow Depth: 0.17 cm

			110	an naw	oounco				
Particle Diameter (Microns)	5.46	6.87	8.66	10.9	13.7	17.3	21.8	27.5	34.6
Mean Master Count	7960	3993	5140	4388	4775	3943	3395	1550	548
Distance Down Slope (cm)	e								
0.64	518	213	129	41	160	237	252	281	125
2.54	493	211	72	73	110	174	209	233	74
5.08	303	136	70	64	82	161	147	134	50
7.62	292	124	71	35	93	75	107	83	31
10.16	299	89	55	67	45	68	84	57	22
Total % Retained	23.93	19.36	7.72	6.38	10.26	18.13	23.53	50.84	58.76
Critical Distance (cm)	0.64	0.64	0.64	2.54	0.64	0.64	0.64	0.64	0.64

Run No: 19 Surface: 40-Grade Slope: 3%

Mean Flow Velocity: 11.8 cm/sec Temperature: 11.1 °C

Mean Flow Depth: .23 cm

Particle Diameter (Microns)	5.46	6.87	8.66	10.9	13.7	17.3	21.8	27.5	34.6
Mean Master Count	8975	5868	4518	5803	5010	5310	4443	2128	638
Distance Down Slope (cm)	e								
0.64	235	108	41	44	51	71	92	77	43
2.54	400	200	52	37	7.2	178	175	154	79
5.08	280	95	20	45	88	111	125	95	32
7.62	305	114	71	78	116	79	100	69	31
Total % Retained	14.04	8.81	4.07	3.52	6.53	8.27	11.07	18.56	29.00
Critical Distance (cm)	2.54	2.54	7.62	7.62	7.62	2.54	2.54	2.54	2.54

Run No: 20 Surface: 40-Grade Slope: 3%

Mean Flow Velocity: 9.6 cm/sec Temperature: 11.1 °C

Mean Flow Depth: .18 cm

			110	ean Naw	Counts				
Particle Diameter (Microns)	5.46	6.87	8.66	10.9	13.7	17.3	21.8	27.5	34.6
Mean Master Count	8720	5140	4843	5963	5445	5798	4078	1698	495
Distance Down Slope (cm)	2								
0.64	364	139	64	67	84	156	189	138	72
2.54	356	154	101	72	101	147	219	203	76
5.08	280	138	77	70	91	121	197	131	56
7.62	305	147	18	49	92	95	124	86	26
Total % Retained	14.97	11.25	5.37	4.33	6.76	8.95	17.88	32.86	46.46
Critical Distance (cm)	0.64	2.54	2.54	2.542.	54	0.64	2.54	2.54	2.54

Run No: 21 Surface: 40-Grade SlopeL 1%

Mean Flow Velocity: 8.7 cm/sec Temperature: 11.1 °C

Mean Flow Depth: .27 cm

			11	can han	countre				
Particle Diameter (Microns)	5.46	6.87	8.66	10.9	13.7	17.3	21.8	27.5	34.6
Mean Master Count	7813	5613	5303	6103	5475	5050	3718	1748	525
Distance Down Slope (cm)	e								
0.64	405	182	124	120	159	150	233	155	70
2.54	400	226	73	201	254	335	341	235	96
5.08	489	246	89	132	233	243	225	163	46
7.62	262	126	82	86	104	108	127	83	25
Total % Retained	19.92	13.90	6.94	8.83	13.70	16.55	24.91	36.38	45.14
Critical Distance (cm)	5.08	5.08	5.08	2.54	2.54	2.54	2.54	2.54	2.54

Run No: 22 Surface: 40-Grade SlopeL 1%

Mean Flow Velocity: 7.7 cm/sec Temperature: 11.1 °C

Mean Flow Depth: .24 cm

mean	Kaw	Counts

Particle Diameter (Microns)	5.46	6.87	8.66	10.9	13.7	17.3	21.8	27.5	34.6
Mean Master Count	8315	4013	4578	5205	5725	5105	4358	1895	555
Distance Down Slop (cm)	e								
0.64	939	438	207	226	346	691	863	639	268
2.54	981	407	221	425	620	706	813	495	155
5.08	569	206	190	247	288	376	400	205	68
7.62	333	118	92.	167	101	159	123	62	20
Total % Retained	34.00	29.13	15.51	20.46	23.67	37.85	50.46	73.93	92.07
Critical Distance (cm)	2.54	0.64	2.54	2.54	2.54	2.54	0.64	0.64	0.64

Run No: 23 Surface: Glass Slope: 5%

Mean Flow Velocity: 13.5 cm/sec Temperature: 11.4 °C

Mean Flow Depth: .11 cm

Particle Diameter (Microns)	5.46	6.87	8.66	10.9	13.7	17.3	21.8	27.5	34.6
Mean Master Count	7958	4043	4738	4020	4693	4045	3295	1445	458
Distance Down Slope (cm)	e								
5.07	96	6	39	20	15	21	13	2	1
7.62	189	61	41	20	90	126	130	55	10
10.16	349	191	67	92	197	244	297	205	54
12.70	377	177	105	92	162	195	234	173	61
15.24	328	107	76	103	146	136	163	117	53
17.78	279	134	77	89	118	137	113	80	35
20.32	281	135	76	94	109	135	142	81	32
22.86	201	69	49	24	53	57	45	30	9
Total % Retained	26.40	21.77	11.19	13.28	18.96	25.98	34.51	51.42	55.67
Critical Distance (cm)	12.70	10.16	12.70	15.40	10.16	10.16	10.16	10.16	12.70

Run No: 24 Surface: 80-Grade Slope: 3%

Mean Flow Velocity: 14.6 cm/sec Temperature: 11.1 °C

Mean Flow Depth: 0.19 cm

			Me	an Raw	Counts				
Particle Diameter (Microns)	5.46	6.87	8.66	10.9	13.7	17.3	21.8	27.5	34.6
Mean Master Count	8875	4575	4570	5545	5170	5075	3635	1743	520
Distance Down Slope (cm)	e								
2.54	422	224	100	62	202	204	249	166	56
5.08	399	142	86	105	132	138	177	134	66
7.62	458	185	107	143	142	244	209	170	64
10.16	269	141	62	71	112	116	126	81	40
12.70	386	136	99	39	118	161	133	99	32
15.24	247	102	75	73	64	87	108	56	24
17.78	436	118	118	153	116	122	132	78	17
20.32	467	195	89	150	125	134	107	72	27
Total % Retained	34.75	27.17	16.10	14.34	19.67	23.76	34.14	49.11	62.69
Critical Distance (cm)	7.62	2.54	7.62	7.62	7.62	7.62	2.54	7.62	5.08

Run No: 25 Surface: 40-Grade Slope: 1%

Mean Flow Velocity: 8.5 cm/sec Temperature: 11.4 °C

Mean Flow Depth: 0.28 cm

Particle Diameter (Microns)	5.46	6.87	8.66	10.9	13.7	17.3	21.8	27.5	34.6
Mean Master Count	7990	2858	5143	5060	6015	5225	3773	1578	508
Distance Down Slope (cm)	e								
0.64	396	223	134	131	157	266	370	227	99
2.54	523	258	175	138	247	328	474	391	158
5.08	328	125	101	114	184	164	185	113	34
7.62	164	104	111	126	97	151	117	76	27
Total % Retained	17.66	24.84	10.13	10.06	11.39	17.40	30.37	50.50	62.60
Critical Distance (cm)	2.54	2.54	2.54	2.54	2.54	2.54	2.54	2.54	2.54

MICHIGAN STATE UNIVERSITY LIBRARIES
3 1293 03175 4884